International Journal of Biological Macromolecules

Effect of thermal annealing and filler ball-milling on the properties of highly filled polylactic acid/pecan (Carya illinoinensis) nutshell biocomposites

--Manuscript Draft--

Manuscript Number:	IJBIOMAC-D-21-05664R2
Article Type:	Research Paper
Section/Category:	Carbohydrates, Natural Polyacids and Lignins
Keywords:	Polylactic acid (PLA), Pecan nutshell (PNS), Biocomposites, Lignocellulosic materials, Ball milling, Thermal annealing
Corresponding Author:	SARAI AGUSTIN, Ph. D. Institute of Polymers Composites and Biomaterials National Research Council: Istituto dei Polimeri Compositi e Biomateriali Consiglio Nazionale delle Ricerche Pozzuoli, Naples ITALY
First Author:	SARAI AGUSTIN, Ph. D.
Order of Authors:	SARAI AGUSTIN, Ph. D.
	Marco Ricciulli, Bachelor
	Veronica Ambrogi, Ph. D.
	Pierfrancesco Cerruti, Ph. D.
	Gennaro Scarinzi, Ph. D.
Abstract:	Biodegradable polymer composites reinforced with agri-food lignocellulosic biowaste represent cost-effective and sustainable materials potentially able to replace traditional composites for structural, household, and packaging applications. Herein, the preparation of polylactic acid (PLA)/pecan nutshell (PNS) biocomposites at high filler loading (50 wt.%) is reported. Moreover, the effect of two environmentally friendly physical treatments, namely ball-milling of the filler and thermal annealing on biocomposites, were evaluated. PNS enhanced the thermal stability, the viscoelastic response, and the crystallinity of the polymer. Furthermore, filler ball-milling also increased the melt fluidity of the biocomposites, potentially improving melt processing. Finally, the presence of PNS remarkably enhanced the effect of thermal annealing in the compounds. In particular, heat deflection temperature of the biocomposites dramatically increased, up to 60 °C with respect to the non-annealed samples. Overall, these results emphasize the potential of combining natural fillers and environmentally benign physical treatments to tailor the properties of PLA biocomposites, especially for those applications which require a stiff and light material with low deformability.
Suggested Reviewers:	Anna Raffaela Matos Costa, Ph. D. Postdoctoral fellow, Federal University of Pernambuco raffaela_matos@yahoo.com.br Dr. Cosa is an expert in composites and composites characterization
	Donatella Duraccio, Ph. D. Researcher, Istituto di Tecnologie Avanzate per l'Energia e la Mobilità Sostenibili donatella.duraccio@stems.cnr.it Dr. Duraccio is an expert on polylactic acid nanocomposites for food packaging applications
	Rodrigo Ortega Toro, Ph. D. Researcher, Universidad de Cartagena rortegap1@unicartagena.edu.co Dr. Ortega is an expert in thermoplastics, biodegradable polymers and their characterization
	Aitor Barrio Ulanga, Ph. D. Researcher, Tecnalia Innovation aitor.barrio@tecnalia.com

Powered by Editorial Manager® and ProduXion Manager® from Aries Systems Corporation

	Dr. Barrio is an expert in chemistry and polymeric materials
	Aleksandra Nesic, Ph. D. Researcher, University of Belgrade: Univerzitet u Beogradu anesic@vin.bg.ac.rs Dr. Nesic is an expert in polymers characterization
	Arash Moeini, Ph. D. Postdoctoral fellow, Technical University of Munich: Technische Universitat Munchen arash.moeini@tum.de Dr. Moeini is an expert in synthesis and characterization of polymers and composites
Opposed Reviewers:	
Response to Reviewers:	

Powered by Editorial Manager® and ProduXion Manager® from Aries Systems Corporation

Manuscript File (Word Document ONLY)

Consiglio Nazionale delle Ricerche
Istituto per i Polimeri, Compositi e Biomateriali
IPCB ISTITUTO PER I POLIMERI COMPOSITI E BIOMATERIALI

Dear Editor, Dr. Yangchao Luo

Please find enclosed the revised version of our manuscript titled “Effect of thermal annealing and filler ball milling on the properties of highly filled polylactic acid/pecan (Carya illinoinensis) nutshell biocomposites” by Sarai Agustin-Salazar, Marco Ricciulli, Veronica Ambrogi, Pierfrancesco Cerruti, and Gennaro Scarinzi.

As you may notice from the attached pdf file highlighting the changes made, the manuscript has been thoroughly revised according to the reviewer advice, and all main points have been addressed. All grammatical and spelling errors have been corrected, and several sentences have been deleted to improve flow and readability of the manuscript. We hope that the manuscript is now suitable for publication in IJBM as a regular article.

We look forward to hearing from you at your earliest convenience.

Sincerely yours,

Sarai Agustin Salazar, on behalf of the authors.

Via Campi Flegrei, 34 - 80078 Pozzuoli (NA)
Telefono +39 081 8675076 - +39 081 8661446 - fax +39 081 8675230 - e-*mail: segreteria@ipcb.cnr.it*

Dear Reviewer,

Once again, we thank you for your time in revising this document.

Comments from

Reviewer #2: Dear Authors,

I suggest to revise the entire document.

I have found some points in your manuscript that must be revised and corrected.

Some of these points are related with wordy sentences, word choice, intricate text, punctuation in compound/complex sentences, etc.

R: the entire manuscript as well as the SI, have been thoroughly revised according to the reviewer advice, and all main points have been addressed.

The references must be uniformized (for instance, ref 54 and ref 61). Similar observation is given in Supporting information, references 5 and 6 are repeated, and ref. 10 is incomplete.

R: all references, in the main manuscript as well as in SI, were corrected.

The manuscript cannot be accepted in this version.

Sincerely,

The reviewer

R: Finally, all grammatical and spelling errors have been corrected, and several sentences have been deleted to improve flow and readability of the manuscript. A pdf file, highlighting the changes made, is included.

Sincerely, the authors.

Highlights

- PNS is a sustainable filler to develop cost-effective PLA biocomposites
- PNS enhanced PLA thermal stability, viscoelastic response, and crystallinity
- High filler loading did not cause significant decay in mechanical properties
- Ball milling of PNS further improved PLA thermal properties and melt fluidity
- Thermal annealing enhanced HDT, stiffness and strength of biocomposites

Manuscript File (Word Document ONLY)

Abstract

Biodegradable polymer composites reinforced with agri-food lignocellulosic biowaste represent cost-effective and sustainable materials potentially able to replace traditional composites for structural, household, and packaging applications. Herein, the preparation of polylactic acid (PLA)/pecan nutshell (PNS) biocomposites at high filler loading (50 wt.%) is reported. Moreover, the effect of two environmentally friendly physical treatments, namely ball-milling of the filler and thermal annealing on biocomposites, were evaluated.

PNS enhanced the thermal stability, the viscoelastic response, and the crystallinity of the polymer. Furthermore, filler ball-milling also increased the melt fluidity of the biocomposites, potentially improving melt processing. Finally, the presence of PNS remarkably enhanced the effect of thermal annealing in the compounds. In particular, heat deflection temperature of the biocomposites dramatically increased, up to 60 °C with respect to the non-annealed samples. Overall, these results emphasize the potential of combining natural fillers and environmentally benign physical treatments to tailor the properties of PLA biocomposites, especially for those applications which require a stiff and light material with low deformability.

Manuscript File (Word Document ONLY) Click here to view linked References

Effect of thermal annealing and filler ball-milling on the properties of highly filled polylactic acid/pecan (*Carya illinoinensis*) nutshell biocomposites

Sarai Agustin-Salazar[1,2,*], Marco Ricciulli[3], Veronica Ambrogi[3], Pierfrancesco Cerruti[4,*], Gennaro Scarinzi[1]

[1]Institute for Polymers, Composites and Biomaterials (IPCB-CNR), Via Campi Flegrei 34, 80078 Pozzuoli (Na), Italy
[2]Department of Chemical and Metallurgical Engineering (DIQyM), University of Sonora, Building 5B, Del Conocimiento, Centro, C.P. 83000, Hermosillo, Sonora, México
[3]University of Naples Federico II, Department of Chemical, Materials and Production Engineering (DICMAPI), Piazzale Tecchio 80, 80125 Naples, Italy
[4]Institute for Polymers, Composites and Biomaterials (IPCB-CNR), Via Gaetano Previati, 1/E, 23900 Lecco, Italy

*Corresponding authors
Sarai Agustin-Salazar, e-mail: sarai.agustin@ipcb.cnr.it
Pierfrancesco Cerruti, email: pierfrancesco.cerruti@cnr.it

Abstract

Biodegradable polymer composites reinforced with agri-food lignocellulosic biowaste represent cost-effective and sustainable materials potentially able to replace traditional composites for structural, household, and packaging applications. Herein, the preparation of polylactic acid (PLA)/pecan nutshell (PNS) biocomposites at high filler loading (50 wt.%) is reported. Moreover, the effect of two environmentally friendly physical treatments, namely ball-milling of the filler and thermal annealing on biocomposites, were evaluated.

PNS enhanced the thermal stability, the viscoelastic response, and the crystallinity of the polymer. Furthermore, filler ball-milling also increased the melt fluidity of the biocomposites, potentially improving melt processing. Finally, the presence of PNS remarkably enhanced the effect of thermal annealing in the compounds. In particular, heat deflection temperature of the biocomposites dramatically increased, up to 60 °C with respect to the non-annealed samples. Overall, these results emphasize the potential of combining natural fillers and environmentally benign physical treatments to tailor the properties of PLA biocomposites, especially for those applications which require a stiff and light material with low deformability.

Keywords

Polylactic acid (PLA), Pecan nutshell (PNS), Biocomposites, Lignocellulosic materials, Ball-milling, Thermal annealing

1. Introduction

A great amount of petro-plastic is used in the preparation of products with a short lifespan. This produces a huge quantity of plastic waste, which creates a remarkable environmental problem. Recycling, incineration, and landfilling are often limited by issues related to the decay of the materials properties, production of greenhouse gases, and shortage of disposal sites, respectively. In this respect, biodegradable or compostabile bioplastics, which are produced from renewable resources, represent a viable alternative to petro-plastics [1].

One of the most important members of the bioplastics family is polylactic acid (PLA), an aliphatic polyester that can be synthesized from reactants derived from natural sources. In addition, PLA is fully biodegradable, and its decomposition products are non-toxic. Due to its good mechanical properties, high stiffness, and biodegradability, PLA is considered as a valuable substitute for various non-biodegradable plastics such as polyethylene (PE), polystyrene (PS), and polyethylene terephthalate (PET) [2]. However, it also has several shortcomings that limit its broader use, such as low crystallization rate, low glass transition temperature (T_g), and brittleness [3,4]. These features negatively affect the physical and mechanical performance of the polymer, which shows sensitivity to ageing at ambient conditions and a low heat deflection temperature (HDT). Therefore, PLA cannot be used to produce items designed for hot food or beverages. To overcome this issue, nucleating agents can be added during processing to improve the crystallization properties [5]. Alternatively, post-process thermal annealing may favor crystallization and stabilize the morphology of the polymer, thus resulting in improved HDT and rigidity [5–8].

High cost also limits the use of PLA as a commodity polymer [4,9]. A viable solution for this shortcoming is the use of cheap fillers in PLA-based products. Among them, lignocellulosic agri-food wastes represent a useful source of very cheap fillers for the preparation of low-cost biocomposites [10–15]. In addition, their use valorizes the feedstock, avoiding its disposal by landfilling or incineration, also relieving the environmental burden relative to these practices. In the last few years, pecan nutshell (PNS) has been proposed as an effective filler to modify mechanical and rheological properties of PLA biocomposites [9,12,16,17]. However, results have been reported for biocomposites loaded with maximum of 30 wt.% filler, and no information on the effect of filler size on the properties of the biocomposites has been provided. In this regard, ball-milling has been successfully applied to reduce particle size of lignocellulosic fillers in polymer composites [18–22]. This technique is based on relatively inexpensive and easy to use equipment and does not require the use of hazardous solvents or reactants. In particular, the effect of filler size has been studied in HDPE composites charged with ball-milled wood fibers [18], which increased the flexural modulus and the melt flow rate (MFR). The latter is a relevant result for the processing of composites with techniques such as injection molding, where high fluidity is required. However, in spite of these examples, the use of ball-milled lignocellulose fillers in PLA-based composites has not been extensively studied, especially at high biomass loading [23–25].

Therefore, in the present paper PLA biocomposites filled with 50 wt.% ball–milled PNS were prepared, and the effect of filler ball-milling time was investigated through spectroscopic, morphological, thermal, rheological and mechanical characterizations of the biomass and the

resulting biocomposites. Further, the effect of filler ball-milling on the thermo-mechanical properties of thermally annealed biocomposites was assessed, with the aim of producing biocomposites with low ageing sensitivity and high heat deflection temperature (HDT).

2. Experimental Section

2.1. Raw materials

PNS was obtained from Asociación Productora de Nuez S.P.R. de R.I (Hermosillo, Mexico). Biomass was ground by a blade mill, sorted through a 250 μm sieve, and stored in dark in hermetically sealed bags at -20 °C. PNS was extracted with ethanol at 80 °C, recovered by filtering on paper, dried at 60 °C, and stored in ziplock bags. The ethanol extracted biomass is referred to as NS1 from here on. The PLA used was Ingeo™ 2003D (94% L isomer), purchased from NatureWorks (NE, USA). Absolute ethanol was obtained from Sigma-Aldrich (Steinheim-Germany).

2.2. Ball-milling of the biomass

NS1 was ball-milled in a Retsch PM100 planetary ball-milling device (Haan, Germany), using a 125 mL steel milling cup and steel spheres (10 mm diameter) [26]. The spheres/NS1 weight ratio was about 10:1. Ball-milling was performed at 650 rpm, and the processing times adopted alongside the corresponding identification codes are shown in Table 1.

2.3. Biocomposites preparation

PLA and biomass (50% wt.) were dried overnight at 60 ºC under vacuum. The formulations (Table 1) were compounded in a twin-screw micro extruder equipped with intermeshing counter-rotating conical screws (HAAKE MiniLab, Thermo Fisher Scientific, Karlsruhe, Germany). The temperature adopted was 170 °C, and the screw speed was maintained at 50 rpm [12]. The obtained strand was pelletized, and square plates (thickness = 3.0 mm, length = 100 mm) were prepared by compression molding using a Collin P20E platen press (Ebersberg, Germany), at 170 ºC (2 min at 0 bar, 1 min at 50 bar, and 2 min at 150 bars). The molded plates were then cooled to room temperature by circulating cold water in the platens. To improve the biocomposites thermomechanical properties, the samples were subjected to thermal annealing at 75 ºC for 72 h in an oven [5–8].

Table 1. Ball-milling (BM) times adopted, coding of the filler and the corresponding PLA biocomposites, and their bulk density.

BM time (min)	Filler codes	Composite codes	Bulk density (g cm^{-3}) *
-	-	PLA	1.10 ± 0.22
0	NS1	PN1	1.12 ± 0.06
30	NS2	PN2	1.10 ± 0.19
60	NS3	PN3	1.26 ± 0.10

120	NS4	PN4	1.10 ± 0.06

*average of 3 measurements. Values are not statistically different.

2.4. Characterization of the materials

2.4.1. Bulk Density

The bulk density of PLA and biocomposites was determined by the liquid displacement method using hexane [27]. The test was performed in triplicate and the resulting values are reported in Table 1.

2.4.2. Thermogravimetric Analysis (TGA)

TGA was performed under both nitrogen and air atmosphere (flow rate 30 mL min^{-1}) using 7 ± 2 mg sample, by a Pyris Diamond TG-DTA analyzer (Perkin Elmer, USA). The analysis protocol included a preliminary drying step at 100 °C for 20 min and a subsequent heating program, from 100 ºC to 800 °C at a rate of 10 ºC min^{-1} [12]. The onset degradation temperature (T_{onset}) was evaluated as the temperature corresponding to the 5% weight loss in the TGA curves. The temperature of maximum degradation rate (T_{max}) was calculated as the temperature corresponding to the maximum of the peak in the derivative thermogravimetric (DTG) plot.

2.4.3. Differential Scanning Calorimetry (DSC)

Calorimetric analyses were performed with a TA DSC-Q2000 instrument under a 50 mL min^{-1} nitrogen flow. Samples (7 ± 2 mg) were first heated from 30 to 180 °C at 5 °C min^{-1}, then cooled down to -30 °C at 5 °C min^{-1} and reheated up to 200 °C at 5 °C min^{-1}. Glass transition temperature (T_g), cold crystallization enthalpy and temperature (ΔH_c, T_c), melting enthalpy and temperature (ΔH_m, T_m) were determined from the first heating scan. A double melting peak was observed, which correspond to the α' and α crystalline forms of PLA [28]. The respective contributions to the melting enthalpy were calculated using the peak analyzer featured in OriginPro 2015 software. Percent crystallinity (χ_c) of PLA and biocomposites, before and after annealing, were calculated from DSC data, according to the following equation:

$$\chi_c\ (\%) = \frac{\Delta Hm}{\Delta H_m^{\circ} \times wt} \times 100 \qquad (1)$$

where the values of ΔH_m (melting enthalpy) and ΔH_m° (melting enthalpy of the 100% crystalline PLA) were considered according to the crystalline form, α'or α. ΔH_m° values used were 107 J g^{-1} for α', and 143 J g^{-1} for α crystalline form [28]. wt was the relative amount of PLA, corresponding to 1 or 0.5 in neat PLA and the biocomposites, respectively.

2.4.4. Fourier Transform Infrared Spectroscopy

FTIR spectra of PNS powder derivatives were carried out by means of a Perkin Elmer Spectrum 100 spectrophotometer (USA), equipped with a Universal ATR diamond crystal sampling accessory. Spectra were recorded as an average of 16 scans, with a resolution of 4 cm^{-1}. FTIR

analysis of annealed PLA and biocomposites was carried out in transmission mode (16 scans, 4 cm^{-1}) on 100 μm thick films obtained by compression molding (1 min at 170 ºC and 50 bar, and 2 min at 170 ºC and 150 bars, and quenching in cold water). The analysis was performed for a maximum of 150 h annealing time. The conversion from the amorphous to the crystalline form of the polymer in the biocomposites was followed by analyzing the ratio of the integrated absorbance of the peaks at 923 cm^{-1} (increasing) and 950 cm^{-1} (decreasing) by the following equation [29]:

$$Conversion = \frac{A_{923}}{A_{950}} \quad (2)$$

where A_{923} is the area of the peak at 923 cm^{-1}, and A_{950} is the area of the peak at 950 cm^{-1}.

2.4.5. Dynamic Light Scattering (DLS)

DLS was used to determine the size distribution of the PNS derivatives after the ball-milling treatment. A Zetasizer Nano ZS instrument (Malvern Instruments, UK) equipped with a 4 mV He-Ne laser operating at λ = 633 nm was used, with a measurement angle of 173°. The analysis was carried out at 25 °C, by suspending 5 mg of biomass in 2 mL of water, and then vortexing the suspension before the analysis [18,30,31].

2.4.6. Rheological analysis and Melt Flow Rate (MFR)

Rheological measurements were carried out by a Thermo Fisher RS6000 (Haake, Germany) stress-controlled rotational rheometer in the dynamic flow field, using parallel plate geometry (diameter = 20 mm). Samples were loaded in the rheometer under nitrogen flow. The gap size between plates was set at 1 mm. The plates were approached (in 120 s) from a gap size of 2.5 mm to the set value. Dynamic frequency sweep tests were performed at 185 °C, with a deformation of 1%, which was well within the linear viscoelastic behavior, over the range of 300 – 0.1 rad s^{-1} from high to low frequency.

MFR of molten PLA and biocomposites (4 ± 1 g) was measured on pellets dried at 60 ºC overnight using a Ceast MF 20 Melt Flow Tester (Instron, model 724 MFM, Italy) at 190 ºC and 2.16 kg load (ASTM D 1238-01e1) [19,32].

2.4.7. Heat Deflection Temperature (HDT)

Heat deflection temperature under load was measured by a Thermo Fisher RS6000 (Haake, Germany) rotational rheometer in uniaxial compression mode, using parallel plate geometry (plate diameter = 20 mm). The specimens (3 × 10 × 50 mm^3) were placed on two metal supports (20 mm span length) and loaded flatwise, with midway constant stress of 0.45 MPa, at a 2 °C min^{-1} heating rate (ASTM E2092). The HDT was calculated as the temperature at which the specimen deformation was equal to 0.25 mm, which corresponded to a 3% strain. The percent strain (%D) was obtained by the following equation:

$$\%D = \frac{(\boldsymbol{d0}-\boldsymbol{d})}{\boldsymbol{d0}} \times 100 \quad (3)$$

where d_0 is the initial rheometer gap (from the plate bottom to the top of the system showed in Fig. S1) and *d is* the final gap.

2.4.8. Scanning Electron Microscopy (SEM)

SEM analysis was carried out by means of a FEI Quanta 200 FEG scanning electron microscope in high vacuum mode. The observations were performed on sputtered samples with an Au-Pd layer. For the PNS derivatives, the observations were carried out on the powder obtained after ball-milling. For the compression molded composite samples the analysis was carried out on the cross-section surfaces of cryofractured samples.

2.4.9. Mechanical tests

The flexural properties of PLA and its biocomposites were determined on specimens (3 × 10 × 100 mm^3) using an Instron model 4505 dynamometer (USA), with a deformation speed of 1 mm min^{-1} and a 48 mm span length (ASTM D 638). For impact tests, a 3.5 mm V-notch was machined on the same specimens, and the tests were performed using a Ceast M197 Charpy pendulum (Ceast, Italy) of potential energy equal to 3.5 J and impact speed of 1 m s^{-1} (ASTM D256). Ahead of measurement, the specimens were conditioned at 25 °C and 50% relative humidity (RH) for 5 days, and the experimental data are an average of 5 determinations [12].

3. Results and discussion

3.1. Characterization of NS and its derivatives

3.1.1. Structural characterization

PNS was first treated with ethanol to recover valuable polyphenolic substances that can be used as functional additives in polymer compounding and other formulations [17,33]. Among alcohols, ethanol is considered economically viable and environmentally safe. It is used to extract substances with a low molecular weight such as phenolic compounds [33–35], and was recently recommended as a green solvent in oil extraction [36,37].

The FTIR spectrum of the biomass after extraction (NS1) is reported in Fig. S2a. Compared with the parent NS, an intensity reduction in the hydroxyl region around 3300 cm^{-1} was noticed. Similarly, a remarkable intensity decrease was detected for the signals correlated to the C–H stretching vibrations of methylene (2923 cm^{-1}) and methyl groups (2855 cm^{-1}). This decrease is related to the removal of the extractable fraction of PNS [16,38]. Conversely, the peaks at 1730 and 1281 cm^{-1} showed a slight increase. These signals are related to the C=O stretching vibrations of the acetyl moieties and C-H deformation of the holocellulose fraction of NS, respectively [12,17], and were comparatively higher in NS1 because of the removal of the ethanol extractable matter.

The effect of ball-milling on the biomass was followed by FTIR analysis (full IR spectra are reported in Fig. S2b in SI). After ball-milling, the spectra showed several changes with the treatment time (Fig. 1). In the carbonyl region, the intensity of the C=O stretching signal at 1730 cm^{-1} (Fig. 1a), as well as that at 1029 cm^{-1} (Fig. 1d), ascribed to secondary alcohols, aliphatic

ethers, or β-(1→4) linkages [39], increased remarkably. On the other hand, the absorption at 1190 cm^{-1} due to the pyranose ring C-O bonds [40] abruptly decreased (Fig. 1c). This evidence indicates that the mechanochemical treatment favored the cleavage of the polysaccharide fraction from the lignocellulosic biomass as well as the occurrence of oxidation reactions. Other changes were noticed in the aromatic skeletal vibration (1604 cm^{-1}) and fingerprint regions of the spectrum (Fig. S2b). In particular, a strong decrease in the absorption peaks at 1280 cm^{-1} (Fig. 1 b) accounted for the amorphization of the cellulose fraction, as also reported for ball-milled spruce wood and cotton cellulose [41,42].

3.1.2. Morphological and size characterization

Figure 2 shows the SEM images of the biomass before and after 30 minutes of milling. Neat NS1 exhibited two main morphologies, consisting of elongated structures and irregularly shaped particles. A more detailed view of the former revealed the complex fibrous structure of well-preserved vascular bundles, consisting of an arrangement of parallelly aligned spiral cellulose microfibrils embedded in a thin cohesive matrix made of lignin and hemicellulose [12]. After 30 minutes of treatment (NS2) there was almost no trace of the fibrillar and spiral-arranged fractions, and only irregularly shaped particles were visible, with dimensions ranging from 1 to 10 μm.

This outcome paralleled the disappearance of the peak at 1280 cm^{-1} (Fig. 1b) in the milled samples as a result of the reduction of the crystalline structures by ball-milling [12,38,40,42]. Higher magnification images showed that the length of the fibrils of pristine biomass dropped to a few microns, and the smaller particles tended to agglomerate (Fig. S3). This was probably caused by the complex structure of lignocellulose and the higher surface energy associated with size reduction. By increasing the ball-milling time to 120 min, the shape and dimensions of the particles remained almost unchanged [43]. This last observation could be attributed to strong hydrogen bonding and van der Waals forces in the complex structure of the biomass [44].

To get further insight on the effect of ball-milling on the size distribution, the biomass was characterized by Dynamic Light Scattering (DLS). Fig. S4 shows the DLS curves at different milling extents. Before ball-milling, the average size of the biomass was well above the instrumental detection limit (10 μm). Therefore, no measurement could be recorded for NS1. A 30 minute milling dramatically reduced the average size of the biomass, as a distribution peak of 2.7±0.2 μm was determined for NS2. Increasing the ball-milling time to 120 minutes resulted in a

further decrease in size, down to 1.5±0.2 μm for NS4.

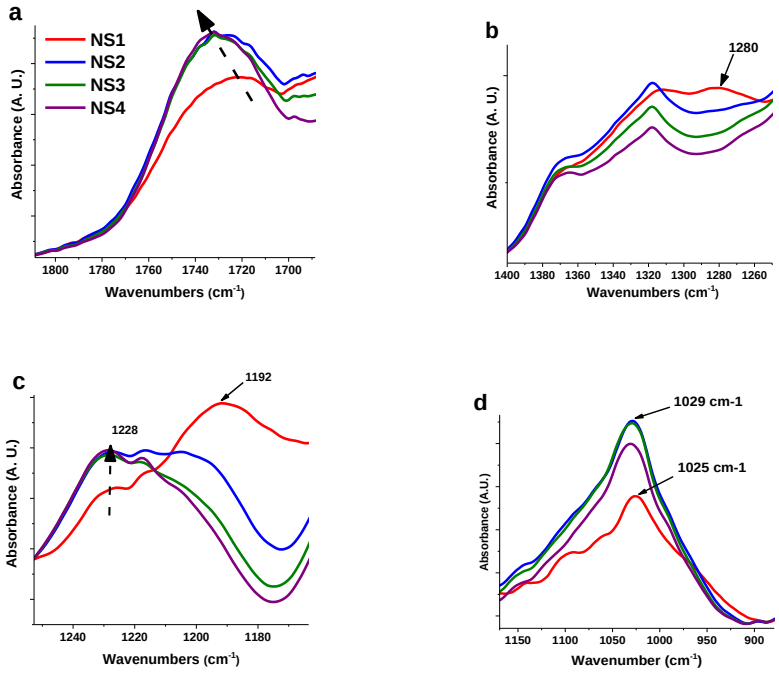

Figure 1. Evolution of FTIR spectra relative to ball-milled biomass at different treatment times. This picture reports the regions where major changes are detected. Full spectra are shown in Fig. S2.

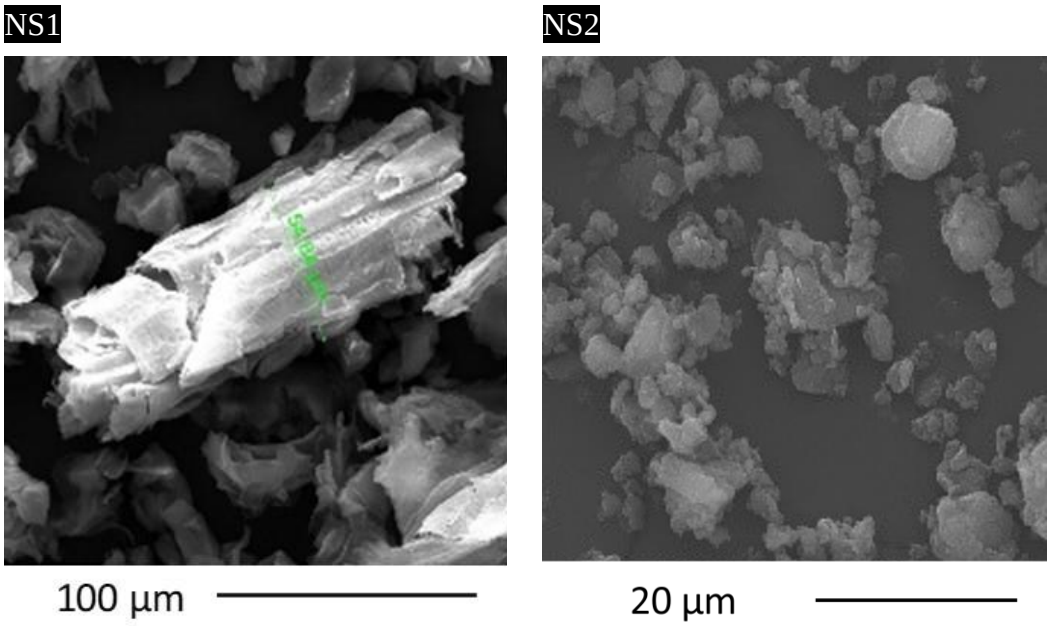

Figure 2. SEM images of NS1 (unmilled) and NS2 (30 min ball-milling).

3.1.3. Thermal analysis

TGA was carried out on PNS derivatives to assess any changes in filler degradation temperature with ball-milling time. TGA curves in nitrogen and the corresponding DTG plots are reported in Fig. S5a in the SI. TGA analyses in air were also carried out (Fig. S5b). In this case, the curves demonstrated an unpredictable behavior at the end of the measurement due to the rapid combustion of the residual char under a 10 ºC min^{-1} heating rate. Therefore, an additional measurement under air atmosphere at 1 ºC $min^{-1}$was performed (Fig. S5c). The corresponding parameters under air are reported in Table S1.

The main TGA parameters are reported in Table 2. Compared with NS1, ball-milling did not affect the shape of the degradation curves, and the mechanochemical treatment scarcely affected the T_{onset} values. T_{max1} showed some change but remained approximately in the value range of the non-ball milled biomass. T_{max2} displayed a decreasing trend with ball-milling time, likely due to the amorphization of the cellulose component. On the contrary, slightly higher residual char values were noticed for the ball-milled samples, as the mechanochemical treatment promoted the dehydration of the biomass, which favored charring. Similar behaviors were reported by Ling et al. [41] on ball-milled cotton, as well as Kim et al. [45] that carried out a TGA study on cotton, tunicate cellulose, and microcrystalline cellulose.

Table 2. TGA data under nitrogen of PNS derivatives at different times of milling (heating rate 10 ºC min^{-1}).

Sample	Nitrogen		
	T_{onset} (ºC)	T_{max} (ºC)	Char. Yield (% wt.) *
NS1	245.6	I) 297.1 II) 363.7	39.7
NS2	245.9	I) 290.5 II) 360.3	40.3
NS3	249.3	I) 295.7 II) 349.2	45.9
NS4	245.8	I) 295.4 II) 349.1	43.4

*at 600ºC. I, and II refer to the first, and second thermo-degradative steps.

3.2. Characterization of PLA biocomposites

3.2.1 Rheology and MFR

The viscoelastic response of pure PLA and PLA biocomposites was investigated to evaluate the effect of the fillers on PLA melt rheology. Dynamic frequency sweep (DFS) tests showed that the polymer melt behavior was mainly viscous (G′<G″) for all samples, and both moduli approached constant values in the rubbery plateau region above 100 rad s^{-1}, where moduli crossover occurred (Figure 3a). The addition of PNS derivatives significantly enhanced the viscoelastic response of PLA, as G′ and G″ values of the biocomposites exceeded those of PLA over the entire frequency range investigated. PN1 exhibited the highest moduli, while the other biocomposites displayed a slight reduction. A plateau in G′ was observed at low frequency for the biocomposites, particularly for PN3 and PN4, indicating the transition from liquid-like to solid-like viscoelastic behavior, which was more marked for the biocomposites containing filler with a smaller size distribution. The complex viscosity curve of pure PLA (Fig. 3b) showed a shear thinning behavior for frequency values higher than 10 rad s^{-1}, and a Newtonian plateau at low frequencies [12]. On the other hand, at low frequency, the biocomposites viscosity curves turned up from the Newtonian plateau. This result can be explained in terms of the formation of a three-dimensional interconnected particulate network in the melt, as well as the restricted mobility of the polymer melt due to the interaction between the polymer chains and filler particles [12,16,17]. Furthermore, PN1 presented the highest complex viscosity, which slightly decreased in the biocomposites charged with the ball-milled biomass, highlighting the importance of the lower size and the shape of the filler after the mechanochemical treatment [46,47].

To gain further insight on this effect, MFR of PLA and PLA-based biocomposites were also measured (Fig. 3c). Melt flow rate values provide information on the processability of the polymeric material through injection molding, extrusion, thermoforming or printing [48]. In polymer composites, MFR values are affected by the load and shape of the filler [20,32] as well as by its interaction with the matrix [19]. In addition, the friction between filler and matrix affects the melt flow. As expected, the presence of filler significantly reduced the MFR value of PN1

(0.55 g min^{-1}) compared to plain PLA (0.85 g min^{-1}), as the interparticle interactions significantly restricted the relative motion between macromolecules [32,49]. Very interestingly, increasing the ball-milling time allowed to recover the melt fluidity. A similar behavior was reported by Gallagher et al. [18], since the reduction of the particle size of wood fiber in maleated polyethylene composites increased the MFR value. Likewise, in biocarbon-filled poly(trimethylene terephthalate) (PTT)/PLA blend composites, the size reduction of the filler particles dramatically reduced the shear viscosity of the composites, which dropped below that of the matrix [49]. The main reasons for the particle size-related decrease in viscosity are the dilution of the polymer chain entanglement density, the selective interaction of polymer chains on the particle surface, and the lower resistance against shear stress [21,49]. Notably, in terms of polymer processability, ball-milling of NS1 made polymer flow and forming procedures easier, hence lowering the energy requirements for manufacturing [50].

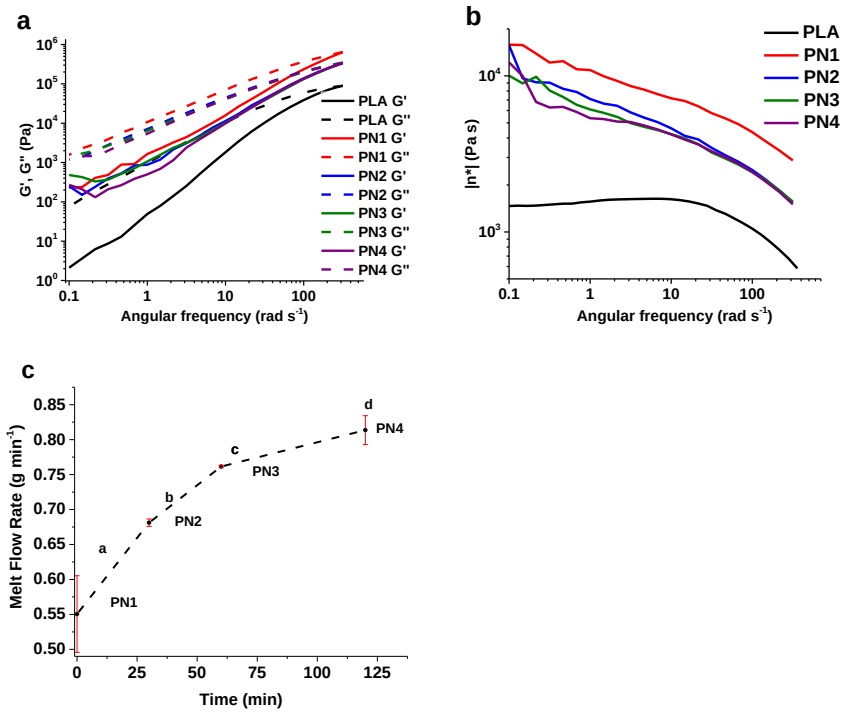

Figure 3. Rheological characterization of PLA and its biocomposites. a) storage and loss moduli (G' and G'', respectively); b) complex viscosity (η^*) vs the angular frequency. c) Relation between Melt flow rate and ball-milling time.

3.2.2. Thermal characterization

The thermal stability of PLA and the prepared biocomposites was assessed by TGA. Thermogravimetric curves obtained under nitrogen are reported in Fig. S6a. Both PLA and its biocomposites exhibited a single-step weight loss process. Neat PLA was characterized by a fast weight drop stage with nearly no char residue. The biocomposites showed a slower degradation process with a residual weight at 600 °C close to 24 wt.% that was independent of the filler ball-

milling duration. Thermogravimetric parameters are reported in Table 3. The T_{onset} of neat PLA was 268.1 °C. Compared to the neat matrix, all biocomposites exhibited higher T_{onset}, especially those containing the ball-milled biomass, with values ranging from 269 °C to 277 °C. As for the temperature of maximum decomposition rate, PLA showed a T_{max} of 304 °C, which increased by nearly 10 °C for PN1 and reached a maximum for PN3 (328.3 °C). The T_{max} improvement of biocomposites can be attributed to a slow thermal degradation rate of the biomass. The effect is more remarkable for samples charged with ball-milled filler due to the finer dispersion of the latter [44]. Summing up, the presence of the biomass increased the thermal stability in inert atmosphere. In particular, the milling treatment of the filler enhanced the T_{max} values (PN3).

TGA measurements were also carried out in air (Fig. S6b). Table S1 in the SI summarizes the calculated thermal parameters. Under air, the higher stability of the biomass contributed to an increase in the T_{max} values of the biocomposites with respect to PLA. The curves and a more detailed discussion are reported in the SI.

Table 3. TGA data of PLA and its biocomposites under nitrogen.

	T_{onset} (ºC)	T_{max} (ºC)	Char. Yield (% wt.)*
PLA	268.1	304.2	2.7
PN1	277.4	312.9	21.6
PN2	269.8	325.8	25.1
PN3	274.7	328.3	24.6
PN4	268.7	319.0	21.4

*at 600ºC.

DSC characterization of PLA and its biocomposites was carried out on the compression molded and annealed samples. Curves related to the first heating scan are shown in Fig. 4 as they are more informative concerning the effects of processing on the properties of the material. All curves showed a change in heat capacity at about 60 °C due to the glass transition, an exothermic peak at around 100 °C due to cold crystallization, and finally the melting endotherm. The latter always appeared as a complex signal featuring two components, related to α'- (147 ºC) and α- (153 ºC) forms, as reported by Cocca et al. [28]. The thermal parameters relative to the DSC traces are listed in Table 4. The T_g was not affected by filler or ball-milling. As for the cold crystallization, PLA exhibited a T_c of 110 °C and a crystallization enthalpy (ΔH_c) equal to 23.6 J g^{-1}. Compared to the plain polyester, all the studied biocomposites showed a shift towards lower temperatures of T_c, that was independent of ball-milling treatment. Regarding the ΔH_c values, PN1 composite (based on non-treated biomass) did not show any change of the parameter. Conversely, biocomposites filled with ball-milled biomass revealed a not negligible improvement of this property. The effect was particularly notable in the PN3 sample (60-min ball-milling) with a ΔH_c value increase of

about 24%, Summarizing, the filler decreased the temperature of cold crystallization, and its nucleating action was more remarkable after ball-milling. Nucleating effects of biobased fillers have been previously reported for PLA/Sisal fibre composites [51], PLA/pecan nutshell [16,17] and other polymeric systems charged with natural fibers [52–54].

The mechanochemical treatment of the filler also affected the melting properties of the biocomposites. As shown in Table 4, the presence of the filler did not affect the T_m relative to the double melting phenomenon but influenced their relative intensity. Furthermore, the total enthalpy of melting (ΔH_m) followed the same trend recorded for ΔH_c. Indeed, PN1 showed the same ΔH_m value as neat PLA (25 J g^{-1}), while biocomposites charged with ball-milled fillers exhibited an improvement in total melting enthalpy. This confirmed the more remarkable nucleating action of the ball-milled biomass. Notably, all the ΔH_m values were slightly higher than the corresponding ΔH_c, indicating that the compression molded samples partly crystallized during cooling. DSC traces relative to the second heating are displayed in Fig. S7a in the SI, and their thermal parameters are shown in Table S2. All the reported curves showed the same experimental features discussed for the first heating run. The same can be said for the values of the experimental parameters.

Among post processing methods established for optimizing the structure and morphology of polymer-based materials, thermal annealing has been commonly used, becoming even indispensable for improving the final product or device performance [5,55]. In the following experiments, the samples were subject to annealing at 75 ºC to improve thermal and mechanical properties of the biocomposites. Fig. 4b displays the first heating DSC curves of PLA and biocomposites after annealing, while the corresponding calorimetric data are reported in Table 4. Remarkably, after the thermal treatment no signal related to the glass transition was noticed, except for PLA, which displayed a T_g increase of about 4 °C compared to the non-annealed counterpart. Besides, none of the samples showed any crystallization exothermal peak, indicating that thermal annealing caused the samples to crystallize. Finally, most of the investigated samples exhibited a single melting endotherm, or possibly a barely visible shoulder on the low temperature side of the peak. In this respect, T_m values were scarcely influenced by sample composition, and fell roughly in between the values of the two melting peaks recorded before annealing. The associated ΔH_m values showed some remarkable effects attributable to the thermal treatment, the presence of the filler and the ball-milling duration. PLA exhibited a ΔH_m equal to 28.8 J g^{-1}, which increased to 32.5 J g^{-1} for PN1, containing the untreated filler. A more remarkable increase of ΔH_m was recorded when the biomass was submitted to ball-milling. The maximum effect was observed after 30 minutes of treatment (sample PN2, 39.5 J g^{-1}), slightly decreasing at higher times. The reported results evidenced the effectiveness of thermal annealing in the morphological stabilization of PLA-based products. In addition, they confirm the role of the biomass as a nucleating agent towards PLA matrix and suggest that ball-milling can significantly improve its action. Finally, the degree of crystallinity (χ_c) was calculated for all samples. Before annealing, PN1 showed a crystallinity similar to neat PLA, while in ball-milled biocomposites this parameter increased at longer milling time. The same behavior was also observed in the samples after annealing.

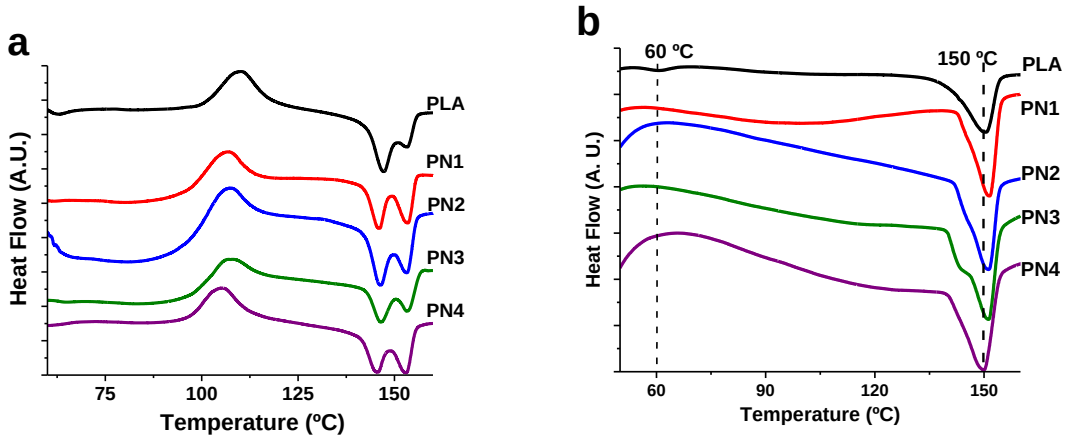

Figure 4. DSC curves (first heating scan) of PLA and its biocomposites, a) before and b) after thermal annealing (at 75 ºC for 72 h).

Table 4. Thermal parameters measured by DSC (first heating scan, 5 °C min^{-1}), for PLA and its biocomposites.

Sample	Before annealing							After annealing[a]			
	T_g (ºC)	T_c (°C)	ΔH_c (J g^{-1})	T_m (ºC)	ΔH_m^{**b} (J g^{-1})	ΔH_m^{*c} (J g^{-1})	χ_c (%)	T_g (ºC)	T_m (ºC)	ΔH_m (J g^{-1})	χ_c (%)
PLA	58.8	110.2	23.6	147.0 153.0	21.5 3.4	24.9	20.1 2.4	62.8	150.5	28.8	23.0
PN1	57.4	106.7	23.7	146.1 153.3	17.4 7.6	25.0	16.2 5.3	-	151.53	32.5	26.0
PN2	61.4	106.7	25.4	146.5 153.0	19.4 6.7	26.0	18.1 4.7	-	151.2	39.5	31.6
PN3	61.5	105.0	29.2	146.8 153.5	23.6 6.3	29.9	22.1 4.4	-	151.3	36.8	29.4
PN4	58.7	105.4	28.7	146.8 153.1	21.4 8.2	29.6	20.0 5.7	-	150	35.1	28.0

[a]performed at 75 ºC for 72 h. [b]the respective contribution of the two melting peaks (related to α'- and α-forms) was calculated. [c]corresponds to the sum of the two peaks.

The effect of thermal annealing on the structure of the investigated samples was further studied by FTIR spectroscopy. The development of crystallinity was assessed by monitoring the absorption band at 923 cm^{-1}, characteristic of the ordered crystalline phase of PLA [56] and attributed to the combination of C–C backbone and CH_3 rocking mode of α crystals [29,57]. Fig. 5a shows the analytical peak upon increasing annealing times for neat PLA. It was noticed that this signal was completely absent before annealing, and progressively rose with the treatment time. Furthermore, the evolution of the signal was fast in the first few hours of treatment and slowed down at longer times. Similar results were obtained for all the biocomposites, as reported for PN1 in Fig. S8 in the SI. The conversion from the amorphous to the crystalline form was quantitatively followed by analyzing the ratio of the integrated absorbance of the peaks at 923 cm^{-1} and 950 cm^{-1} (A_{923}/A_{950}), the latter arising from the amorphous fraction of PLA [29]. The absorbance ratios of the studied samples are reported in Fig. 5b as a function of the annealing time. In all cases most of the crystallization process occurred during the first 24 hours of thermal treatment while after 72 hours a plateau was reached. The latter outcome evidences that at this annealing time, the crystallization process is almost complete, and samples used for bulk characterization were fully crystallized. It was noticed that at low annealing times PN1 exhibited higher conversion rates than PLA. Furthermore, all biocomposites, compared to the neat matrix, reached larger plateau values of the parameter at longer times. This evidence agrees with DSC results, which showed higher crystallinity degrees for composites and further confirmed the nucleating action of the filler towards the thermoplastic matrix. However, no differences in biocomposites crystallinity were noticed by FTIR analysis after the thermal annealing.

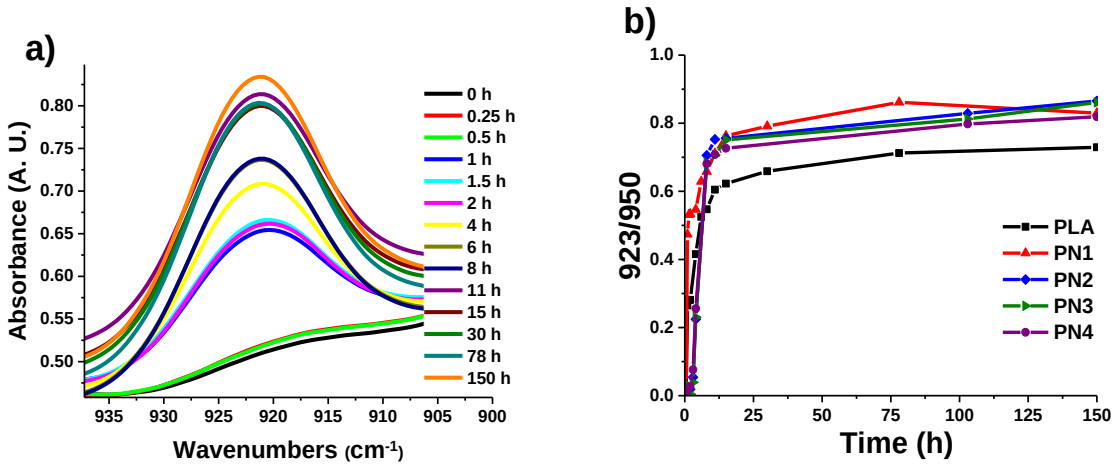

Figure 5. a) Evolution of the 923 cm^{-1} infrared absorption band of neat PLA upon time. b) Conversion progress from amorphous to crystalline form due to annealing followed by A_{923}/A_{950} ratio as a function of the annealing time for PLA and its biocomposites.

3.2.3. Thermomechanical properties

One of the possible applications of biodegradable polymers is to replace their conventional

counterparts for manufacturing disposable plates and cups, which come in contact with hot food or beverages. In this respect, PLA exhibits poor resistance to high temperature and low HDT, that is a measure of the ability of the polymer to bear a given load as a function of temperature. The HDT value of a polymeric material depends on stiffness and glass transition temperature. In addition, in polymer composites, it can be also influenced by filler size distribution, aspect ratio and filler content. Therefore, in the present paper, HDT measurements were carried out to assess the possible influence of filler milling and thermal annealing on this parameter.

The deflection versus temperature plots of the prepared samples before and after annealing are reported in Fig. 6. It is noticed that the prepared biocomposites showed higher deformability with the temperature when compared with plain PLA. This finding is confirmed by the HDT values [58] reported in Table 5. This decay could be due to the presence of filler particles that increase the number of defects at the charge-matrix interface. Moreover, ball-milling of the biomass resulted in further decreased HDT values, likely due to the low aspect ratio of the particles. However, since the PNS derivatives demonstrated to be effective nucleating agents, able to increase PLA crystallinity and in turn to improve its thermomechanical performance, HDT measurements were carried out also on thermally annealed samples.

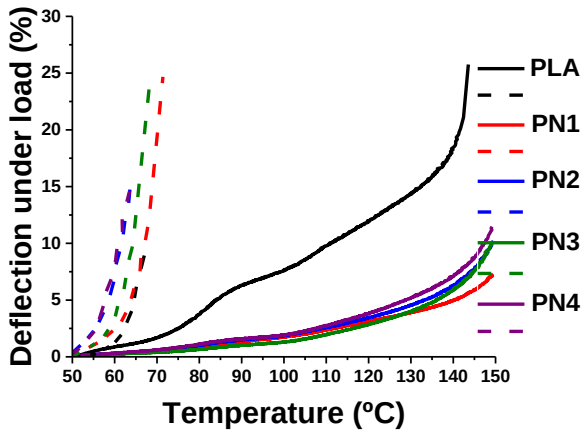

Figure 6. Deflection under load versus temperature for PLA and its biocomposites. Dashed lines: samples before annealing. Solid lines: samples after annealing (at 75 ºC for 72 h).

Table 5. HDT parameters calculated for PLA and its biocomposites.

	Before	After annealing*	
Sample	HDT (°C)	HDT(°C)	Strain at 140 ºC (%)
PLA	63.1	77.1	18.5
PN1	61.0	118.5	5.0
PN2	56.7	114.9	6.3
PN3	59.9	121.6	5.9
PN4	56.2	112.6	7.1

*at 75 ºC for 72 h.

All the annealed samples showed a significant decrease in deformability with respect to the pristine ones, and the effect was dramatically enhanced for the biocomposites. This outcome is even more detectable if the values of strain at 140 °C are considered (Table 5). The value of this parameter was 18.5 % for neat PLA and dropped to 5-7 % in the composite samples. In the same table, HDT values are also reported. By comparing the HDT data of pristine and heat-treated samples, an outstanding improvement of the parameter was noticed. Even in this case, the effect was more remarkable for the biocomposites. Annealed PLA showed a HDT value of 77 °C, with a 14 °C increase with respect the pristine sample. Biocomposites exhibited HDT values ranging from 113 °C to 121 °C, with as nearly as 60 °C improvement compared to the non-annealed samples. This result highlighted the dramatic impact of crystallinity, as measured by DSC and FTIR spectroscopy, on the thermomechanical properties of PLA. The effects of filler loading and annealing on HDT have been reported for PLA [59], PLA blends [55], and composites filled with natural fibers and mineral fillers [51,60,61,62]. As for the thermomechanical behavior of non-annealed PLA composites, most authors report that the presence of the charge scarcely influence HDT values which remains in the range of the plain matrix [51,60], in agreement with our results. However, after annealing, an improvement of thermomechanical performance is often recorded. The effect is detected either on neat PLA and its compounds but is more remarkable for composites [51,60–62] due to the nucleating action of the filler towards the matrix. The development of trans-crystallinity at polymer-matrix interface during annealing can have a role in HDT improvement [51], however, filler dimensions can also affect the HDT performances of the materials [62].

3.*2.4. SEM analysis of cryofractured surfaces*

SEM analysis of the cryogenically fractured surfaces of the PLA and PLA biocomposite plates provided insight on filler distribution and morphological properties of the samples, as well as on the interfacial adhesion between filler and matrix. Micrographs relative to PLA, PN1 and PN2, before and after annealing, are reported in Fig. 7. The corresponding images related to PN3 and PN4 are reported in the SI (Fig. S9). As for non-annealed samples, PLA showed a fracture surface almost featureless typical of glassy polymeric materials. The investigated biocomposites exhibited

a rough and irregularly fractured surface that revealed the inclusion of biomass particles, which appeared to be well dispersed in the polymer matrix. The composite PN1, charged with non-ball-milled biomass, showed the presence of filler particles, with a 15-20 μm dimension range, exhibiting fiber-fracture phenomena. Examination of the matrix-filler interface clearly showed some voids around the particles (delamination), suggesting poor adhesion of the filler to the polymeric phase.

Concerning the effect of the ball-milling, it can be observed that even a 30-minute treatment (PN2 sample) of the biomass resulted in a significantly more homogeneous surface, along with a remarkable reduction of filler domain dimensions with sizes ranging from 15 μm down to 1 μm. It is also noticed that in this case filler fracture was limited to bigger particles, and the prevailing deformation mechanism was fiber pull-out. Longer milling times of the filler did not significantly change the morphology of the fracture surface (PN3 in Fig. S9). The cavities produced by milled PNS particles pull out are clearly visible confirming that the matrix filler interplay between pure PLA and the lignocellulosic filler was not very efficient.

With regards to the fracture surfaces of annealed samples, SEM analysis evidenced that heat treatment scarcely affected the morphology of the studied materials. Compared with the non-annealed specimen, PLA exhibited a rougher surface with a higher number of fracture planes close to each other. The increase in surface roughness was also noticed in the micrographs of the annealed biocomposites and, for PN4 sample (Fig. S9), was so high that the detection of filler particle was no longer possible. Other studies have reported similar effect of the PNS (formation of agglomerates) into PLA, even with lower loadings of filler [16,17].

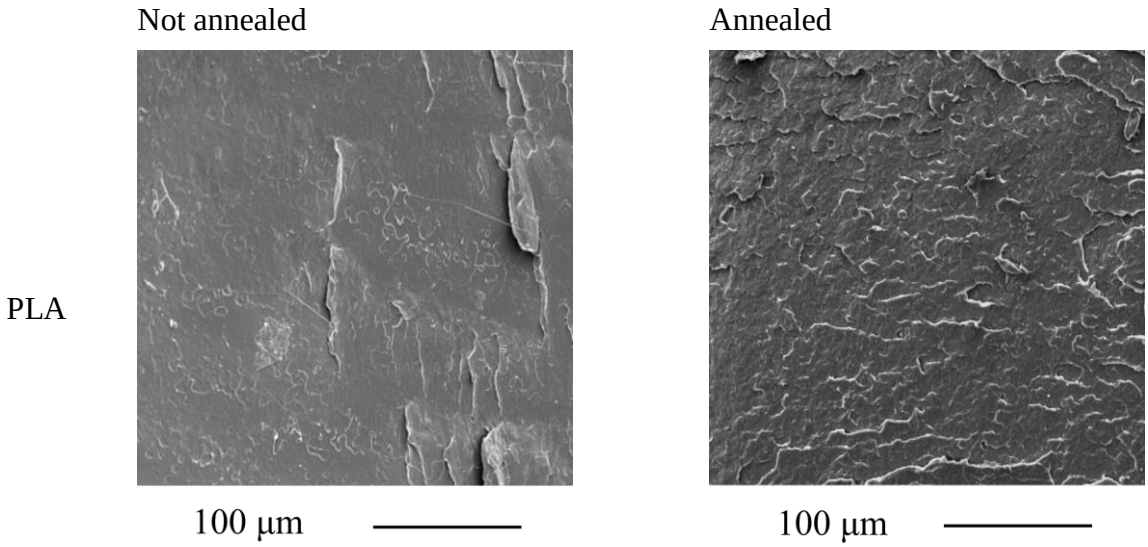

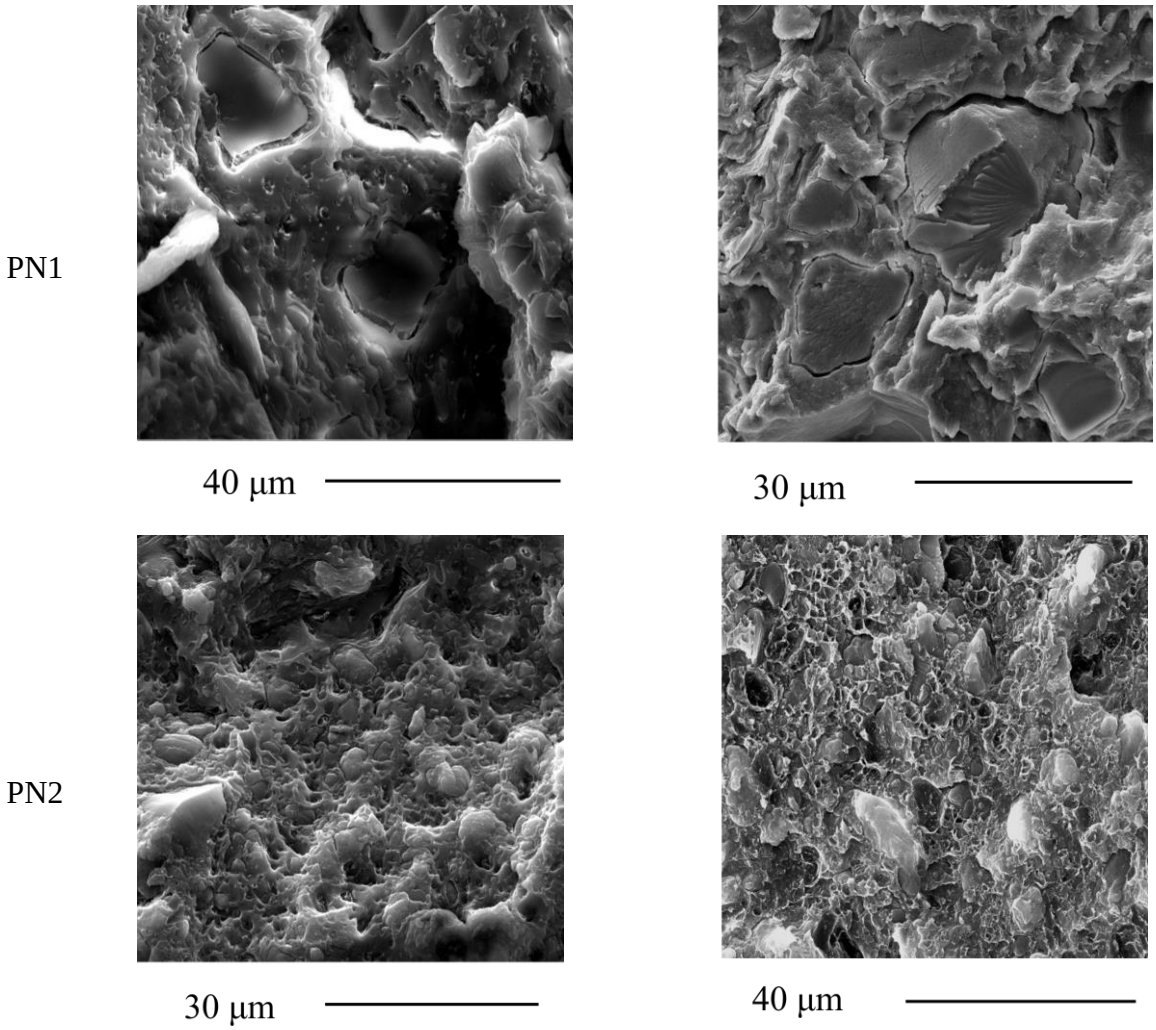

Figure 7. Morphological characterization of PLA and its biocomposites. SEM images of cryofractured surfaces of PLA, PN1, and PN2 before and after annealing (at 75 ºC for 72 h).

3.2.5. Mechanical Properties

The mechanical performance of the pristine and annealed biocomposites was assessed by flexural and impact tests (Table 6). Concerning flexural properties, all the prepared biocomposites showed an enhancement in elastic modulus before annealing with respect to pure PLA. This effect was more significant for PN1, which exhibited a 39% improvement, and less significant for the biocomposites charged with the ball-milled filler. Conversely, the presence of the filler negatively affected the flexural properties of the samples, causing a 30-40 % decrease in stress at break and a more remarkable reduction of strain at break. Impact tests of the investigated biocomposites displayed a drop in toughness with respect to plain PLA. In particular, ball-milling caused resilience to further decrease, attaining less than halved values with respect to the plain polyester. A comparable behavior was noticed for the impact strength, which dropped by about 30% on average. Flexural and impact tests were also performed on samples after annealing. The investigation was carried out on plain PLA and PN1 biocomposite, as the latter was the sample

showing the best properties among the prepared samples. Their flexural data reported in Table 6, show that the heat treatment caused an improvement in both modulus and stress at break with respect the corresponding non-annealed samples. The same was observed for the impact strength but not for the resilience values.

The reported results show that pecan nutshell at 50 % loading improves the flexural modulus of the PLA matrix but the stiffening effect is less efficient if the filler if submitted to ball-milling. The flexural data also show that the presence of the filler produces a reduction of stress and strain at break. The latter outcome was also recorded for the impact results that exhibit a decay of both stress and resilience of the biocomposites compared to neat PLA.

The reduced stiffening action of ball-milled fillers can be ascribed to the mechanochemical treatment that brought about amorphization of the cellulosic fraction of the charge, the reduction of molecular weight of its components and the decrease of its aspect ratio [63]. The decay of flexural stress and strain at break and impact properties can be associated to the scarce interaction between the charge and the continuous polymeric phase, as indicated by SEM analysis. Indeed, it has been reported that in polymer composites the ultimate properties are the most sensitive to the filler-matrix adhesion [64].

However, the stiff nature of the fillers employed in this work can also play a role. A similar decay of properties at break has been reported for PLA biocomposites modified with pecan nutshell, oat husk, cocoa shells and apple pomace, as well as in the PBS/Arboform® system [12,16,17,65].

Table 6. Mechanical properties of PLA and its biocomposites.

	FLEXURAL			IMPACT	
	Stress at break (MPa)	Modulus (MPa)	Strain at break (%)	Strength (N)	Resilience (KJ/m2)
Before annealing					
PLA	82.9±3.7^{d}	3224±291.0^{a}	4.1±0.2^{c}	105.3 ± 5.1^{b}	2.8 ± 0.4^{e}
PN1	55.8±1.5^{b}	4426±166.0^{d,e}	1.3±0.0^{a}	78.3 ± 8.2^{a}	1.2 ± 0.1^{c}
PN2	55.7±0.7^{b}	4337±55.0^{d}	1.3±0.0^{a}	70.5±4.6^{a}	0.9±0.1^{b}
PN3	49.6±0.8^{a}	3937±234.0^{b,c}	1.3±0.1^{a}	61.9±8.4^{a}	0.7±0.1^{a}
PN4	51.2±3.4^{a,b}	4208±159.0^{c,d}	1.2±0.1^{a}	70.3±5.2^{a}	0.8±0.1^{a,b}
After annealing*					
PLA	87.3±8.0^{d}	3631±90.0^{b}	2.8±0.6^{b}	118.0 ± 5.5^{c}	1.9 ± 0.3^{d}
PN1	67.4±7.9^{c}	4691±109.0^{e}	1.5±0.2^{a}	101.5 ± 6.6^{b}	1.1 ± 0.4^{b,c}

^{a}Values with same letter in same column do not present significant difference. *at 75 ^{o}C for 72 h.

As for the effect of annealing on mechanical properties, the improvement of flexural and impact strength data can be associated with the increase of crystallinity produced by the thermal treatment.

Similar effects were reported by Chen et al. [55] for PLA/PLC blends, and by Li et al. [66] on PLA biocomposites reinforced with multi-walled carbon nanotubes.

4. Conclusions

In this study, low density, cost-effective, and potentially highly biodegradable biocomposites have been successfully prepared by charging PLA with a high amount (50 wt.%) of pecan nutshell, usually regarded as an agri-food by-product. The effects of ball-milling of the filler and the annealing of the corresponding biocomposites were investigated.

The introduction of the non-ball milled biomass at high loading into the PLA matrix enhanced the polymer viscoelastic response and decreased the MFR. These effects were attributed to the restricted mobility of the polymer melt and the formation of a three-dimensional interconnected particulate network. The presence of the filler also enhanced the polymer thermal stability due to the slower degradation rate of the lignocellulosic biomass with respect to neat PLA. Furthermore, it acted as a heterogeneous nucleating agent, promoting PLA crystallization. It also affected the mechanical properties by improving flexural modulus, reducing flexural stress and strain at break and impact properties.

Composites charged with ball-milled biomass showed similar features but the effects of the filler on polymer properties were influenced by the mechanochemical treatment applied. Ball-milling of the biomass produced a reduction of particle size along with a deconstruction of the material that involves amorphization, reduction in aspect ratio and mechanical strength. These features affected the properties of the corresponding biocomposites. Indeed, composites based on ball-milled fillers exhibited an increase in MFR and thermal stability, a more pronounced nucleation action, but also a reduction in mechanical properties. Rheological, thermodegradative and morphological effects can be related to the reduction of particle size of the filler while the loss of mechanical properties can be due to its lower mechanical strength.

Finally, thermal annealing increased the mechanical and thermomechanical properties of all materials. In particular, thermal treatment had a dramatic effect the HDT values of the composites that resulted to be on average 50% higher if compared to neat non-annealed PLA.

Overall, these results emphasize the potential of pecan nutshell as a source of sustainable filler to develop cost-effective PLA biocomposites with tailored mechanical properties. These materials could be used when stiff, light, and low deformable products are required, including structural, household, and packaging applications, like food containers, packaging trays, or disposable items.

5. Acknowledgments

Dr. S. Agustin-Salazar thanks to Consejo Nacional de Ciencia y Tecnología (CONACyT- Mexico) for the postdoctoral fellow grant.

Funding from the EU H2020 CE-BG-06-2019 project “Developing and Implementing Sustainability-Based Solutions for Bio-Based Plastic Production and Use to Preserve Land and Sea Environmental Quality in Europe (BIO-PLASTICS EUROPE)” n. 860407, is gratefully

acknowledged.
Funding by Regione Lombardia under the ROP ERDF 2014–2020-Axis I-Call Hub Ricerca e Innovazione, project "sPATIALS3" (ID 1176485), is gratefully acknowledged.

6. References

[1] J. Yu, L.X.L. Chen, The Greenhouse Gas Emissions and Fossil Energy Requirement of Bioplastics from Cradle to Gate of a Biomass Refinery, Environ. Sci. Technol. 42 (2008) 6961–6966. https://doi.org/10.1021/es7032235.

[2] O.M. Sanusi, A. Benelfellah, D.N. Bikiaris, N. Aït Hocine, Effect of rigid nanoparticles and preparation techniques on the performances of poly(lactic acid) nanocomposites: A review, Polym. Adv. Technol. 32 (2021) 444–460. https://doi.org/10.1002/pat.5104.

[3] H. Pilz, B. Brandt, R. Fehringer, The impact of plastics on life cycle energy consumption and greenhouse gas emissions in Europe, n.d. https://www.plasticseurope.org/application/files/9015/1310/4686/september-2010-the-impact-of-plastic.pdf.

[4] J. Pimentel, G. Rodríguez, I. Gil, Synthesis of Alternative Cost-Effective Process Flowsheets for Lactic Acid Valorization by Means of the P-Graph Methodology, Ind. Eng. Chem. Res. 59 (2020) 5921–5930. https://doi.org/10.1021/acs.iecr.9b06555.

[5] L. Duan, Y. Zhang, H. Yi, F. Haque, C. Xu, S. Wang, A. Uddin, Thermal annealing dependent dielectric properties and energetic disorder in PffBT4T-2OD based organic solar cells, Mater. Sci. Semicond. Process. 105 (2020) 104750. https://doi.org/10.1016/j.mssp.2019.104750.

[6] H. Cai, V. Dave, R.A. Gross, S.P. McCarthy, Effects of physical aging, crystallinity, and orientation on the enzymatic degradation of poly(lactic acid), J. Polym. Sci. Part B Polym. Phys. 34 (1996) 2701–2708. https://doi.org/10.1002/(SICI)1099-0488(19961130)34:16<2701::AID-POLB2>3.0.CO;2-S.

[7] K.W. Meereboer, M. Misra, A.K. Mohanty, Review of recent advances in the biodegradability of polyhydroxyalkanoate (PHA) bioplastics and their composites, Green Chem. 22 (2020) 5519–5558. https://doi.org/10.1039/D0GC01647K.

[8] L.-T. Lim, R. Auras, M. Rubino, Processing technologies for poly(lactic acid), Prog. Polym. Sci. 33 (2008) 820–852. https://doi.org/10.1016/j.progpolymsci.2008.05.004.

[9] A. Ahmad, F. Banat, H. Taher, A review on the lactic acid fermentation from low-cost renewable materials: Recent developments and challenges, Environ. Technol. Innov. 20 (2020) 101138. https://doi.org/10.1016/j.eti.2020.101138.

[10] S. Agustin-Salazar, P. Cerruti, G. Scarinzi, 9 Biobased structural additives for polymers, in: Sustain. Polym. Mater., De Gruyter, 2020: pp. 193–234. https://doi.org/10.1515/9783110590586-009.

[11] T. Mukherjee, N. Kao, PLA Based Biopolymer Reinforced with Natural Fibre: A Review, J. Polym. Environ. 19 (2011) 714–725. https://doi.org/10.1007/s10924-011-0320-6.

[12] S. Agustin-Salazar, P. Cerruti, L.Á. Medina-Juárez, G. Scarinzi, M. Malinconico, H. Soto-Valdez, N. Gamez-Meza, Lignin and holocellulose from pecan nutshell as reinforcing fillers in poly (lactic acid) biocomposites, Int. J. Biol. Macromol. 115 (2018) 727–736. https://doi.org/10.1016/j.ijbiomac.2018.04.120.

[13] K.L. Pickering, M.G.A. Efendy, T.M. Le, A review of recent developments in natural

fibre composites and their mechanical performance, Compos. Part A Appl. Sci. Manuf. 83 (2016) 98–112. https://doi.org/10.1016/j.compositesa.2015.08.038.
[14] L. Berglund, M. Noël, Y. Aitomäki, T. Öman, K. Oksman, Production potential of cellulose nanofibers from industrial residues: Efficiency and nanofiber characteristics, Ind. Crops Prod. 92 (2016) 84–92. https://doi.org/10.1016/j.indcrop.2016.08.003.
[15] A. Bartos, K. Nagy, J. Anggono, Antoni, H. Purwaningsih, J. Móczó, B. Pukánszky, Biobased PLA/sugarcane bagasse fiber composites: Effect of fiber characteristics and interfacial adhesion on properties, Compos. Part A Appl. Sci. Manuf. 143 (2021) 106273. https://doi.org/10.1016/j.compositesa.2021.106273.
[16] D. Sánchez-Acosta, A. Rodriguez-Uribe, C.R. Álvarez-Chávez, A.K. Mohanty, M. Misra, J. López-Cervantes, T.J. Madera-Santana, Physicochemical Characterization and Evaluation of Pecan Nutshell as Biofiller in a Matrix of Poly(lactic acid), J. Polym. Environ. 27 (2019) 521–532. https://doi.org/10.1007/s10924-019-01374-6.
[17] C.R. Álvarez-Chávez, D.L. Sánchez-Acosta, J.C. Encinas-Encinas, J. Esquer, P. Quintana-Owen, T.J. Madera-Santana, Characterization of Extruded Poly(lactic acid)/Pecan Nutshell Biocomposites, Int. J. Polym. Sci. 2017 (2017) 1–12. https://doi.org/10.1155/2017/3264098.
[18] L.W. Gallagher, A.G. McDonald, The effect of micron sized wood fibers in wood plastic composites, Maderas. Cienc. y Tecnol. 15 (2013) 0–0. https://doi.org/10.4067/S0718-221X2013005000028.
[19] N. Suaduang, S. Ross, G.M. Ross, S. Pratumshat, S. Mahasaranon, Effect of spent coffee grounds filler on the physical and mechanical properties of poly(lactic acid) bio-composite films, Mater. Today Proc. 17 (2019) 2104–2110. https://doi.org/10.1016/j.matpr.2019.06.260.
[20] T. Huber, M. Misra, A.K. Mohanty, The effect of particle size on the rheological properties of polyamide 6/biochar composites, AIP Conf. Proc. 1664 (2015) 6–10. https://doi.org/10.1063/1.4918500.
[21] Y. Zheng, Z. Fu, D. Li, M. Wu, Effects of ball milling processes on the microstructure and rheological properties of microcrystalline cellulose as a sustainable polymer additive, Materials (Basel). 11 (2018) 1–13. https://doi.org/10.3390/ma11071057.
[22] A. Isa, J. Minamino, Y. Kojima, S. Suzuki, H. Ito, R. Makise, M. Okamoto, T. Endo, The Influence of Dry-Milled Wood Flour on The Physical Properties of Wood Flour/Polypropylene Composites, J. Wood Chem. Technol. 36 (2016) 105–113. https://doi.org/10.1080/02773813.2015.1083583.
[23] C.G. Silva, P.A.L. Campini, D.B. Rocha, D.S. Rosa, The influence of treated eucalyptus microfibers on the properties of PLA biocomposites, Compos. Sci. Technol. 179 (2019) 54–62. https://doi.org/10.1016/j.compscitech.2019.04.010.
[24] V. Baheti, J. Militky, M. Marsalkova, Mechanical properties of poly lactic acid composite films reinforced with wet milled jute nanofibers, Polym. Compos. 34 (2013) 2133–2141. https://doi.org/10.1002/pc.22622.
[25] S. Bhagia, R.R. Lowden, D. Erdman, M. Rodriguez, B.A. Haga, I.R.M. Solano, N.C. Gallego, Y. Pu, W. Muchero, V. Kunc, A.J. Ragauskas, Tensile properties of 3D-printed wood-filled PLA materials using poplar trees, Appl. Mater. Today. 21 (2020) 100832. https://doi.org/10.1016/j.apmt.2020.100832.
[26] R. Avolio, V. Graziano, Y.D.F. Pereira, M. Cocca, G. Gentile, M.E. Errico, V. Ambrogi, M. Avella, Effect of cellulose structure and morphology on the properties of poly(butylene

succinate-co-butylene adipate) biocomposites, Carbohydr. Polym. 133 (2015) 408–420. https://doi.org/10.1016/j.carbpol.2015.06.101.
[27] R. Prem chand, Y.P. Ravitej, K.M. Chandrasekhar, H. Adarsha, J.V. Shivamani kanta, M. Veerachari, R. Ravi kumar, Abhinandan, Characterization of banana and E glass fiber reinforced hybrid epoxy composites, Mater. Today Proc. 46 (2021) 9119–9125. https://doi.org/10.1016/j.matpr.2021.05.402.
[28] M. Cocca, M.L. Di Lorenzo, M. Malinconico, V. Frezza, Influence of crystal polymorphism on mechanical and barrier properties of poly(l-lactic acid), Eur. Polym. J. 47 (2011) 1073–1080. https://doi.org/10.1016/j.eurpolymj.2011.02.009.
[29] N. Vasanthan, O. Ly, Effect of microstructure on hydrolytic degradation studies of poly (l-lactic acid) by FTIR spectroscopy and differential scanning calorimetry, Polym. Degrad. Stab. 94 (2009) 1364–1372. https://doi.org/10.1016/j.polymdegradstab.2009.05.015.
[30] J.B. Engel, M. Mac Ginity, C.L. Luchese, I.C. Tessaro, J.C. Spada, Reuse of Different Agroindustrial Wastes: Pinhão and Pecan Nutshells Incorporated into Biocomposites Using Thermocompression, J. Polym. Environ. 28 (2020) 1431–1440. https://doi.org/10.1007/s10924-020-01696-w.
[31] C.L. Luchese, V.F. Abdalla, J.C. Spada, I.C. Tessaro, Evaluation of blueberry residue incorporated cassava starch film as pH indicator in different simulants and foodstuffs, Food Hydrocoll. 82 (2018) 209–218. https://doi.org/10.1016/j.foodhyd.2018.04.010.
[32] H. Long, Z. Wu, Q. Dong, Y. Shen, W. Zhou, Y. Luo, C. Zhang, X. Dong, Effect of polyethylene glycol on mechanical properties of bamboo fiber-reinforced polylactic acid composites, J. Appl. Polym. Sci. 136 (2019) 3–10. https://doi.org/10.1002/app.47709.
[33] S. Agustin-Salazar, N. Gamez-Meza, L.Á. Medina-Juárez, M. Malinconico, P. Cerruti, Stabilization of Polylactic Acid and Polyethylene with Nutshell Extract: Efficiency Assessment and Economic Evaluation, ACS Sustain. Chem. Eng. 5 (2017). https://doi.org/10.1021/acssuschemeng.6b03124.
[34] S. Agustin-Salazar, L.A. Medina-Juárez, H. Soto-Valdez, F. Manzanares-López, N. Gámez-Meza, Influence of the solvent system on the composition of phenolic substances and antioxidant capacity of extracts of grape (Vitis vinifera L.) marc, Aust. J. Grape Wine Res. 20 (2014) 208–213. https://doi.org/10.1111/ajgw.12063.
[35] F. Manzanarez-López, H. Soto-Valdez, R. Auras, E. Peralta, Release of α-Tocopherol from Poly(lactic acid) films, and its effect on the oxidative stability of soybean oil, J. Food Eng. 104 (2011) 508–517. https://doi.org/10.1016/j.jfoodeng.2010.12.029.
[36] S.L.B. Navarro, C.E.C. Rodrigues, Macadamia oil extraction methods and uses for the defatted meal byproduct, Trends Food Sci. Technol. 54 (2016) 148–154. https://doi.org/10.1016/j.tifs.2016.04.001.
[37] X. Zhuang, Z. Zhang, Y. Wang, Y. Li, The effect of alternative solvents to n-hexane on the green extraction of Litsea cubeba kernel oils as new oil sources, Ind. Crops Prod. 126 (2018) 340–346. https://doi.org/10.1016/j.indcrop.2018.10.004.
[38] F. Moccia, S. Agustin-Salazar, L. Verotta, E. Caneva, S. Giovando, G. D'Errico, L. Panzella, M. D'Ischia, A. Napolitano, Antioxidant properties of agri-food byproducts | and specific boosting effects of hydrolytic treatments, Antioxidants. 9 (2020) 1–22. https://doi.org/10.3390/antiox9050438.
[39] M. Kacuráková, P. Capek, V. Sasinková, N. Wellner, A. Ebringerová, FT-IR study of plant cell wall model compounds: pectic polysaccharides and hemicelluloses, Carbohydr. Polym. 43 (2000) 195–203. https://doi.org/10.1016/S0144-8617(00)00151-X.

[40] L.M. Ilharco, A.R. Garcia, J. Lopes da Silva, L.F. Vieira Ferreira, Infrared Approach to the Study of Adsorption on Cellulose: Influence of Cellulose Crystallinity on the Adsorption of Benzophenone, Langmuir. 13 (1997) 4126–4132. https://doi.org/10.1021/la962138u.
[41] Z. Ling, T. Wang, M. Makarem, M. Santiago Cintrón, H.N. Cheng, X. Kang, M. Bacher, A. Potthast, T. Rosenau, H. King, C.D. Delhom, S. Nam, J. Vincent Edwards, S.H. Kim, F. Xu, A.D. French, Effects of ball milling on the structure of cotton cellulose, Cellulose. 26 (2019) 305–328. https://doi.org/10.1007/s10570-018-02230-x.
[42] M. Schwanninger, J.C. Rodrigues, H. Pereira, B. Hinterstoisser, Effects of short-time vibratory ball milling on the shape of FT-IR spectra of wood and cellulose, Vib. Spectrosc. 36 (2004) 23–40. https://doi.org/10.1016/j.vibspec.2004.02.003.
[43] A.A. Vaidya, L.A. Donaldson, R.H. Newman, I.D. Suckling, S.H. Campion, J.A. Lloyd, K.D. Murton, Micromorphological changes and mechanism associated with wet ball milling of Pinus radiata substrate and consequences for saccharification at low enzyme loading, Bioresour. Technol. 214 (2016) 132–137. https://doi.org/10.1016/j.biortech.2016.04.084.
[44] A. Solikhin, Y.S. Hadi, M.Y. Massijaya, S. Nikmatin, Novel Isolation of Empty Fruit Bunch Lignocellulose Nanofibers Using Different Vibration Milling Times-Assisted Multimechanical Stages, Waste and Biomass Valorization. 8 (2017) 2451–2462. https://doi.org/10.1007/s12649-016-9765-0.
[45] U.J. Kim, S.H. Eom, M. Wada, Thermal decomposition of native cellulose: Influence on crystallite size, Polym. Degrad. Stab. 95 (2010) 778–781. https://doi.org/10.1016/j.polymdegradstab.2010.02.009.
[46] E.O. Ogunsona, M. Misra, A.K. Mohanty, Composites : Part A Impact of interfacial adhesion on the microstructure and property variations of biocarbons reinforced nylon 6 biocomposites, Compos. Part A. 98 (2017) 32–44. https://doi.org/10.1016/j.compositesa.2017.03.011.
[47] Y. Zheng, Z. Fu, D. Li, M. Wu, Effects of Ball Milling Processes on the Microstructure and Rheological Properties of Microcrystalline Cellulose as a Sustainable Polymer Additive, Materials (Basel). 11 (2018) 1057. https://doi.org/10.3390/ma11071057.
[48] O. Olejnik, A. Masek, J. Zawadziłło, Processability and Mechanical Properties of Thermoplastic Polylactide/Polyhydroxybutyrate (PLA/PHB) Bioblends, Materials (Basel). 14 (2021) 898. https://doi.org/10.3390/ma14040898.
[49] V. Nagarajan, A.K. Mohanty, M. Misra, Biocomposites with Size-Fractionated Biocarbon: Influence of the Microstructure on Macroscopic Properties, ACS Omega. 1 (2016) 636–647. https://doi.org/10.1021/acsomega.6b00175.
[50] V. Mazzanti, F. Mollica, A review of wood polymer composites rheology and its implications for processing, Polymers (Basel). 12 (2020) 1–23. https://doi.org/10.3390/polym12102304.
[51] A. Orue, A. Eceiza, A. Arbelaiz, The effect of sisal fiber surface treatments, plasticizer addition and annealing process on the crystallization and the thermo-mechanical properties of poly(lactic acid) composites, Ind. Crops Prod. 118 (2018) 321–333. https://doi.org/10.1016/j.indcrop.2018.03.068.
[52] L. Běhálek, M. Maršálková, P. Lenfeld, J. Habr, J. Bobek, M. Seidl, Study Of Crystallization Of Polylactic Acid Composites And Nanocomposites With Natural Fibres By Dsc Method, in: NANOCON 2013. 5th Int. Conf., Technical University of Liberec,

Brno, Czech Republic., 2013: pp. 1–6.
[53] L. Ferry, G. Dorez, A. Taguet, B. Otazaghine, J.M. Lopez-Cuesta, Chemical modification of lignin by phosphorus molecules to improve the fire behavior of polybutylene succinate, Polym. Degrad. Stab. 113 (2015) 135–143. https://doi.org/10.1016/j.polymdegradstab.2014.12.015.
[54] T. Tábi, S. Hajba, J.G. Kovács, Effect of crystalline forms (α′ and α) of poly(lactic acid) on its mechanical, thermo-mechanical, heat deflection temperature and creep properties, Eur. Polym. J. 82 (2016) 232–243. https://doi.org/10.1016/j.eurpolymj.2016.07.024.
[55] J. Chen, C. Deng, R. Hong, Q. Fu, J. Zhang, Effect of thermal annealing on crystal structure and properties of PLLA/PCL blend, J. Polym. Res. 27 (2020) 221. https://doi.org/10.1007/s10965-020-02206-1.
[56] V. Di Lisio, E. Sturabotti, I. Francolini, A. Piozzi, A. Martinelli, Effects of annealing above Tg on the physical aging of quenched PLLA studied by modulated temperature FTIR, J. Polym. Sci. Part B Polym. Phys. 57 (2019) 174–181. https://doi.org/10.1002/polb.24769.
[57] J. Zhang, Y. Duan, H. Sato, H. Tsuji, I. Noda, S. Yan, Y. Ozaki, Crystal Modifications and Thermal Behavior of Poly(L-lactic acid) Revealed by Infrared Spectroscopy, Macromolecules. 38 (2005) 8012–8021. https://doi.org/10.1021/ma051232r.
[58] I. ASTM, ASTM D648-18, Standard Test Method for Deflection Temperature of Plastics Under Flexural Load in the Edgewise Position, (2018) 14. https://doi.org/10.1520/D0648-18.
[59] G. Li, B. Yang, W. Han, H. Li, Z. Kang, J. Lin, Tailoring the thermal and mechanical properties of injection- molded poly (lactic acid) parts through annealing, J. Appl. Polym. Sci. 138 (2021) 49648. https://doi.org/10.1002/app.49648.
[60] Q.F. Shi, H.Y. Mou, Q.Y. Li, J.K. Wang, W.H. Guo, Influence of heat treatment on the heat distortion temperature of poly(lactic acid)/bamboo fiber/talc hybrid biocomposites, J. Appl. Polym. Sci. 123 (2012) 2828–2836. https://doi.org/10.1002/app.34807.
[61] R.A. Bubeck, A. Merrington, A. Dumitrascu, P.B. Smith, Thermal analyses of poly(lactic acid) PLA and micro-ground paper blends, J. Therm. Anal. Calorim. 131 (2018) 309–316. https://doi.org/10.1007/s10973-017-6466-2.
[62] J. Wootthikanokkhan, T. Cheachun, N. Sombatsompop, S. Thumsorn, N. Kaabbuathong, N. Wongta, J. Wong-On, S.I. Na Ayutthaya, A. Kositchaiyong, Crystallization and thermomechanical properties of PLA composites: Effects of additive types and heat treatment, J. Appl. Polym. Sci. 129 (2013) 215–223. https://doi.org/10.1002/app.38715.
[63] J. Móczó, B. Pukánszky, Polymer micro and nanocomposites: Structure, interactions, properties, J. Ind. Eng. Chem. 14 (2008) 535–563. https://doi.org/10.1016/j.jiec.2008.06.011.
[64] B. Pukánszky, Influence of interface interaction on the ultimate tensile properties of polymer composites, Composites. 21 (1990) 255–262. https://doi.org/10.1016/0010-4361(90)90240-W.
[65] D. Battegazzore, S. Bocchini, J. Alongi, A. Frache, Plasticizers, antioxidants and reinforcement fillers from hazelnut skin and cocoa by-products: Extraction and use in PLA and PP, Polym. Degrad. Stab. 108 (2014) 297–306. https://doi.org/10.1016/j.polymdegradstab.2014.03.003.
[66] M.X. Li, S.H. Kim, S.W. Choi, K. Goda, W. Il Lee, Effect of reinforcing particles on hydrolytic degradation behavior of poly (lactic acid) composites, Compos. Part B Eng. 96

(2016) 248–254. https://doi.org/10.1016/j.compositesb.2016.04.029.

Author statement

Individual contributions:

Marco Ricciulli. Investigation, Writing-Original draft.
Veronica Ambrogi. Writing-Original draft, Visualization.
Pierfrancesco Cerruti. Methodology, Validation, Formal analysis, Resources, Writing-Original draft, Writing-Review & editing, Visualization, Supervision, Funding acquisition.
Gennaro Scarinzi. Methodology, Resources, Data curation, Writing-Original draft, Writing-Review & editing.
Sarai Agustin-Salazar. Conceptualization, Validation, Formal analysis, Investigation, Writing-Original draft, Writing-Review & editing, Visualization, Supervision, Project administration.

Manuscript File (Word Document ONLY)

Click here to access/download
Supplementary Material
Agustin-Salazar et al. SI.docx

Manuscript File (Word Document ONLY) Click here to view linked References

Effect of thermal annealing and filler ball-milling on the properties of highly filled polylactic acid/pecan (*Carya illinoinensis*) nutshell biocomposites

Sarai Agustin-Salazar[1,2,*], Marco Ricciulli[3], Veronica Ambrogi[3], Pierfrancesco Cerruti[4,*], Gennaro Scarinzi[1]

[1]Institute for Polymers, Composites and Biomaterials (IPCB-CNR), Via Campi Flegrei 34, 80078 Pozzuoli (Na), Italy

[2]Department of Chemical and Metallurgical Engineering (DIQyM), University of Sonora, Building 5B, Del Conocimiento, Centro, C.P. 83000, Hermosillo, Sonora, México

[3]University of Naples Federico II, Department of Chemical, Materials and Production Engineering (DICMAPI), Piazzale Tecchio 80, 80125 Naples, Italy

[4]Institute for Polymers, Composites and Biomaterials (IPCB-CNR), Via Gaetano Previati, 1/E, 23900 Lecco, Italy

*Corresponding authors
Sarai Agustin-Salazar, e-mail: sarai.agustin@ipcb.cnr.it
Pierfrancesco Cerruti, email: pierfrancesco.cerruti@cnr.it

Abstract

Biodegradable polymer composites reinforced with agri-food lignocellulosic biowaste represent cost-effective and sustainable materials potentially able to replace traditional composites for structural, household, and packaging applications. Herein, the preparation of polylactic acid (PLA)/pecan nutshell (PNS) biocomposites at high filler loading (50 wt.%) is reported. Moreover, the effect of two environmentally friendly physical treatments, namely ball-milling of the filler and thermal annealing on biocomposites, were evaluated.

PNS enhanced the thermal stability, the viscoelastic response, and the crystallinity of the polymer. Furthermore, filler ball-milling also increased the melt fluidity of the biocomposites, potentially improving melt processing. Finally, the presence of PNS remarkably enhanced the effect of thermal annealing in the compounds. In particular, heat deflection temperature of the biocomposites dramatically increased, up to 60 °C with respect to the non-annealed samples. Overall, these results emphasize the potential of combining natural fillers and environmentally benign physical treatments to tailor the properties of PLA biocomposites, especially for those applications which require a stiff and light material with low deformability.

Keywords

Polylactic acid (PLA), Pecan nutshell (PNS), Biocomposites, Lignocellulosic materials, Ballmilling, Thermal annealing

1. Introduction

A great amount of petro-plastic is used in the preparation of products with a short lifespan. This produces a huge quantity of plastic waste, which creates a remarkable environmental problem. Recycling, incineration, and landfilling are often limited by issues related to the decay of the materials properties, production of greenhouse gases, and shortage of disposal sites, respectively. In this respect, biodegradable or compostabile bioplastics, which are produced from renewable resources, represent a viable alternative to petro-plastics [1].

One of the most important members of the bioplastics family is polylactic acid (PLA), an aliphatic polyester that can

Eliminato:
Eliminato: charge
Eliminato: .%),
Eliminato:
Eliminato:
Eliminato: PNS as a source of sustainable filler
Eliminato: mechanical
Eliminato: ,
Eliminato:

be synthesized from reactants derived from natural sources. In addition, PLA is fully biodegradable, and its decomposition products are non-toxic. Due to its good mechanical properties, high stiffness, and biodegradability, PLA is considered as a valuable substitute for various non-biodegradable plastics such as polyethylene (PE), polystyrene (PS), and polyethylene terephthalate (PET) [2]. However, it also has several shortcomings that limit its broader use, such as low crystallization rate, low glass transition temperature (T_g), and brittleness [3,4]. These features negatively affect the physical and mechanical performance of the polymer, which shows sensitivity to ageing at ambient conditions and a low heat deflection temperature (HDT). Therefore, PLA cannot be used to produce items designed for hot food or beverages. To overcome this issue, nucleating agents can be added during processing to improve the crystallization properties [5]. Alternatively, post-process thermal annealing may favor crystallization and stabilize the morphology of the polymer, thus resulting in improved HDT and rigidity [5–8]. High cost also limits the use of PLA as a commodity polymer [4,9]. A viable solution for this shortcoming is the use of cheap fillers in PLA-based products. Among them, lignocellulosic agrifood wastes represent a useful source of very cheap fillers for the preparation of low-cost biocomposites [10–15]. In addition, their use valorizes the feedstock, avoiding its disposal by landfilling or incineration, also relieving the environmental burden relative to these practices. In the last few years, pecan nutshell (PNS) has been proposed as an effective filler to modify mechanical and rheological properties of PLA biocomposites [9,12,16,17]. However, results have been reported for biocomposites loaded with maximum of 30 wt.% filler, and no information on the effect of filler size on the properties of the biocomposites has been provided. In this regard, ball-milling has been successfully applied to reduce particle size of lignocellulosic fillers in polymer composites [18–22]. This technique is based on relatively inexpensive and easy to use equipment and does not require the use of hazardous solvents or reactants. In particular, the effect of filler size has been studied in HDPE composites charged with ball-milled wood fibers [18], which increased the flexural modulus and the melt flow rate (MFR). The latter is a relevant result for the processing of composites with techniques such as injection molding, where high fluidity is required. However, in spite of these examples, the use of ball-milled lignocellulose fillers in PLAbased composites has not been extensively studied, especially at high biomass loading [23–25]. Therefore, in the present paper PLA biocomposites filled with 50 wt.% ball–milled PNS were prepared, and the effect of filler ball-milling time was investigated through spectroscopic, morphological, thermal, rheological and mechanical characterizations of the biomass and the

Eliminato: Nowadays, plastic materials are widely utilized in every aspect of daily life. Almost all plastics (99%) are obtained from fossil raw materials (petro-plastics), and their preparation is energy intensive, involving the emission of greenhouse gases [1].

Eliminato: materials'

Eliminato: ¶
Bioplastics

Eliminato: defined as materials

Eliminato: endowed with the properties of biodegradability and compostability. They are considered

Eliminato: valuable

Eliminato: , in order to limit their environmental issues

Eliminato: [2].

Eliminato: One of the most important members of the bioplastics family is polylactic acid (PLA), an aliphatic polyester that can be synthesized from reactants derived from natural sources. In addition, PLA is fully biodegradable, and its decomposition products are non-toxic. Due to its good mechanical properties, high stiffness and biodegradability, PLA has been proposed as a valuable substitute of several non-biodegradable plastics such as polyethylene (PE), polystyrene (PS) and polyethylene terephthalate (PET) [3]. However, it also has several shortcomings that limit its broader use, such as low crystallization rate, low glass transition temperature (T_g), and brittleness [4,5]. These features negatively affect the physical and mechanical performance of the material, which shows sensitivity to ageing at ambient conditions and a low heat deflection temperature (HDT). The low HDT value means that PLA cannot be used to produce items designed for hot food or beverages. To overcome this issue, the most common strategy is to improve the crystallization properties with the addition of nucleating agents during processing [6]. Alternatively, post-process thermal annealing may favor crystallization and stabilize the morphology of the polymer, thus resulting in improved HDT and rigidity [6–9].¶ High cost also limits the use of PLA as a commodity polymer [5,10]. A viable solution for this shortcoming is the use of cheap fillers in PLA-based products. Among them, lignocellulosic agri-food wastes represent a useful source of very cheap fillers for the preparation of low cost biocomposites [11–16]. In addition, their use valorizes the feedstock, avoiding its disposal by landfilling or incineration, and lessens the environmental burden relative to these practices. In the last few years, pecan nutshell (PNS) has been proposed as an effective filler to modify mechanical and rheological properties of PLA biocomposites [10,17–19]. However, results have been reported for biocomposites loaded with maximum 30 wt.% filler, and no information on the effect of filler size on the properties of the biocomposites has been provided. In this regard, ball milling has been successfully applied to reduce particle size of lignocellulosic fillers in polymer composites [20–24]. This technique is based on relatively inexpensive and easy to use equipment and does not require the use of

hazardous solvents or ...

resulting biocomposites. Further, the effect of filler ball-milling on the thermo-mechanical properties of thermally annealed biocomposites was assessed, with the aim of producing biocomposites with low ageing sensitivity and high heat deflection temperature (HDT).

2. Experimental Section

2.1. Raw materials

PNS was obtained from Asociación Productora de Nuez S.P.R. de R.I (Hermosillo, Mexico). Biomass was ground by a blade mill, sorted through a 250 μm sieve, and stored in dark in hermetically sealed bags at -20 °C. PNS was extracted with ethanol at 80 °C, recovered by filtering on paper, dried at 60 °C, and stored in ziplock bags. The ethanol extracted biomass is referred to as NS1 from here on. The PLA used was Ingeo™ 2003D (94% L isomer), purchased from NatureWorks (NE, USA). Absolute ethanol was obtained from Sigma-Aldrich (SteinheimGermany).

2.2. Ball-milling of the biomass

Eliminato: NS1 was ball-milled in a Retsch PM100 planetary ball-milling device (Haan, Germany), using a Eliminato: 125 mL steel milling cup and steel spheres (10 mm diameter) [26]. The spheres/NS1 weight ratio Eliminato:

was about 10:1. Ball-milling was performed at 650 rpm, and the processing times adopted Eliminato: [28]. The spheres/NS1 weight ratio was about alongside the corresponding identification codes are shown in Table 1. 10:1. Ball

Eliminato: sieved

Eliminato: in the absence of light

Eliminato: reported

2.3. Biocomposites preparation

PLA and biomass (50% wt.) were dried overnight at 60 ºC under vacuum. The formulations (Table 1) were compounded in a twin-screw micro extruder equipped with intermeshing counter-rotating conical screws (HAAKE MiniLab, Thermo Fisher Scientific, Karlsruhe, Germany). The temperature adopted was 170 °C, and the screw speed was maintained at 50 rpm [12]. The obtained strand was pelletized, and square plates (thickness = 3.0 mm, length = 100 mm) were prepared by compression molding using a Collin P20E platen press (Ebersberg, Germany), at 170 ºC (2 min at 0 bar, 1 min at 50 bar, and 2 min at 150 bars). The molded plates were then cooled to room temperature by circulating cold water in the platens. To improve the biocomposites thermomechanical properties, the samples were subjected to thermal annealing at 75 ºC for 72 h

Bulk density

Eliminato: [19].

30	NS2	PN2	1.10 ± 0.19
60	NS3	PN3	1.26 ± 0.10

in an oven [5–8].

Codice campo modificato

Eliminato: 6–9

Table 1. Ball-milling (BM) times adopted, coding of the filler and the corresponding PLA biocomposites, and their bulk density.

Eliminato:

BM time (min)	Filler codes	Composite codes	(g cm^{-3}) *
-	-	PLA	1.10 ± 0.22
0	NS1	PN1	1.12 ± 0.06
120	NS4	PN4	1.10 ± 0.06

*average of 3 measurements. Values are not statistically different.

2.4. Characterization of the materials

2.4.1. Bulk Density

The bulk density of PLA and biocomposites was determined by the liquid displacement method using hexane [27]. The test was performed in triplicate and the resulting values are reported in Table 1.

2.4.2. Thermogravimetric Analysis (TGA)

TGA was performed under both nitrogen and air atmosphere (flow rate 30 mL min^{-1}) using 7 ± 2 mg sample, by a Pyris Diamond TG-DTA analyzer (Perkin Elmer, USA). The analysis protocol included a preliminary drying step at 100 °C for 20 min and a subsequent heating program, from 100 ºC to 800 °C at a rate of 10

ºC min^{-1} [12]. The onset degradation temperature (T_{onset}) was evaluated as the temperature corresponding to the 5% weight loss in the TGA curves. The temperature of maximum degradation rate (T_{max}) was calculated as the temperature corresponding to the maximum of the peak in the derivative thermogravimetric (DTG) plot.

2.4.3. Differential Scanning Calorimetry (DSC)

Calorimetric analyses were performed with a TA DSC-Q2000 instrument under a 50 mL min^{-1} nitrogen flow. Samples (7 ± 2 mg) were first heated from 30 to 180 °C at 5 °C min^{-1}, then cooled down to -30 °C at 5 °C min^{-1} and reheated up to 200 °C at 5 °C min^{-1}. Glass transition temperature (T_g), cold crystallization enthalpy and temperature (ΔH_c, T_c), melting enthalpy and temperature (ΔH_m, T_m) were determined from the first heating scan. A double melting peak was observed, which correspond to the α' and α crystalline forms of PLA [28]. The respective contributions to the melting enthalpy were calculated using the peak analyzer featured in OriginPro 2015 software. Percent crystallinity (χ_c) of PLA and biocomposites, before and after annealing, were calculated from DSC data, according to the following equation:

analysis of annealed PLA and biocomposites was carried out in transmission mode (16 scans, 4 cm^{-1}) on 100 μm thick films obtained by compression molding (1 min at 170 ºC and 50 bar, and 2 min at 170 ºC and 150 bars, and quenching in cold water). The analysis was performed for a maximum of 150 h annealing time. The conversion from the amorphous to the crystalline form of the polymer in the biocomposites was followed by analyzing the ratio of the integrated absorbance of the peaks at 923 cm^{-1} (increasing) and 950 cm^{-1} (decreasing) by the following equation [29]:

$$CCCCCCCCCCCCCCCCCCCC = {}^{AA}{}_{AA}{}^{923} \quad (2)$$
$$\Delta HHHH$$

$$\chi\chi_{cc}\,(\%) = \frac{\Delta HH^{mm\circ} \times wwww}{} \times 100 \quad (1)$$

where the values of ΔHH_{HH} (melting enthalpy) and ΔHH_{HH}° (melting enthalpy of the 100% crystalline PLA) were considered according to the crystalline form, α'or α. ΔHH_{HH}° values used were 107 J g^{-1} for α', and 143 J g^{-1} for α crystalline form [28]. wt was the relative amount of PLA, corresponding to 1 or 0.5 in neat PLA and the biocomposites, respectively.

2.4.4. Fourier Transform Infrared Spectroscopy

FTIR spectra of PNS powder derivatives were carried out by means of a Perkin Elmer Spectrum 100 spectrophotometer (USA), equipped with a Universal ATR diamond crystal sampling accessory. Spectra were recorded as an average of 16 scans, with a resolution of 4 cm^{-1}. FTIR

Formattato: Tipo di carattere: +Titoli CS (Times New Roman), 12 pt

Formattato: Titolo 3;Paragrafi, Giustificato, Interlinea: multipla 1,15 ri **Eliminato:** ¶ ¶

¶

¶

¶

¶

Eliminato: [29].

Eliminato: [30].

Eliminato: [19].

Eliminato: of

Eliminato: $\frac{}{\Delta HHHH}$

Eliminato: $\frac{\circ \quad \times}{\Delta HH_{mm} \times wwww_{-\%}}$

Eliminato: α'- or α-. ΔHH_{HH} values are reported in the Table 4.
ΔHH_{HH}° values used were 107 J g^{-1} for α', and 143 J g^{-1} for α crystalline form [30]. wt.% correspond to the PLA mass %.

950 where A_{923} is the area of the peak at 923 cm^{-1}, and A_{950} is the area of the peak at 950 cm^{-1}.

2.4.5. Dynamic Light Scattering (DLS)

DLS was used to determine the size distribution of the PNS derivatives after the ball-milling treatment. A Zetasizer Nano ZS

instrument (Malvern Instruments, UK) equipped with a 4 mV He-Ne laser operating at λ = 633 nm was used, with a measurement angle of 173°. The analysis was carried out at 25 °C, by suspending 5 mg of biomass in 2 mL of water, and then vortexing the suspension before the analysis [18,30,31].

2.4.6. Rheological analysis and Melt Flow Rate (MFR)

Rheological measurements were carried out by a Thermo Fisher RS6000 (Haake, Germany) stresscontrolled rotational rheometer in the dynamic flow field, using parallel plate geometry (diameter = 20 mm). Samples were loaded in the rheometer under nitrogen flow. The gap size between plates was set at 1 mm. The plates were approached (in 120 s) from a gap size of 2.5 mm to the set value. Dynamic frequency sweep tests were performed at 185 °C, with a deformation of 1%, which was well within the linear viscoelastic behavior, over the range of 300 – 0.1 rad s^{-1} from high to low frequency.

MFR of molten PLA and biocomposites (4 ± 1 g) was measured on pellets dried at 60 ºC overnight using a Ceast MF 20 Melt Flow Tester (Instron, model 724 MFM, Italy) at 190 ºC and 2.16 kg load (ASTM D 1238-01e1) [19,32].

2.4.7. Heat Deflection Temperature (HDT)

Heat deflection temperature under load was measured by a Thermo Fisher RS6000 (Haake, Germany) rotational rheometer in uniaxial compression mode, using parallel plate geometry (plate diameter = 20 mm). The specimens (3 × 10 × 50 mm^3) were placed on two metal supports (20 mm span length) and loaded flatwise, with midway constant stress of 0.45 MPa, at a 2 °C min^{-1} heating rate (ASTM E2092). The HDT was calculated as the temperature at which the specimen deformation was equal to 0.25 mm, which corresponded to a 3% strain. The percent strain (%D) was obtained by the following equation:

$$\%DD = \left(\frac{}{dddd - dd_{dddd}}\right) \times 100 \quad (3)$$

Formattato: Tipo di carattere: Corsivo **Eliminato:**

Eliminato: and **Eliminato:**

where d_0 is the initial rheometer gap (from the plate bottom to the top of the system showed in Fig. S1) and *d is* the final gap.

2.4.8. Scanning Electron Microscopy (SEM)

SEM analysis was carried out by means of a FEI Quanta 200 FEG scanning electron microscope in high vacuum mode. The observations were performed on sputtered samples with an Au-Pd

Codice campo modificato

Eliminato: 31

layer. For the PNS derivatives, the observations were carried out on the powder obtained after ball- milling. For the compression molded composite samples the analysis was carried out on the crosssection surfaces of cryofractured samples.

Codice campo modificato

Eliminato: 20,32,33

2.4.9. Mechanical tests

The flexural properties of PLA and its biocomposites were determined on specimens (3 × 10 × 100 mm^3) using an Instron model 4505 dynamometer (USA), with a deformation speed of 1 mm min^{-1} and a 48 mm span length (ASTM D 638). For impact tests, a 3.5 mm V-notch was machined on the same specimens, and the tests were performed using a Ceast M197 Charpy pendulum (Ceast, Italy) of

Eliminato: 21,34

Codice campo modificato

potential energy equal to 3.5 J and impact speed of 1 m s^{-1} (ASTM D256). Ahead of measurement, the specimens were conditioned at 25 °C and 50% relative humidity (RH) for 5 days, and the experimental data are an average of 5 determinations [12].

3. Results and discussion

3.1. Characterization of NS and its derivatives

3.1.1. Structural characterization

PNS was first treated with ethanol to recover valuable polyphenolic substances that can be used as functional additives in polymer compounding and other formulations [17,33]. Among alcohols, ethanol is considered economically viable and environmentally safe. It is used to extract substances with a low molecular weight such as phenolic compounds [33–35], and was recently recommended as a green solvent in oil extraction [36,37].

The FTIR spectrum of the biomass after extraction (NS1) is reported in Fig. S2a. Compared with the parent NS, an intensity reduction in the hydroxyl region around 3300 cm^{-1} was noticed. Similarly, a remarkable intensity decrease was detected for the signals correlated to the C–H stretching vibrations of methylene (2923 cm^{-1}) and methyl groups (2855 cm^{-1}). This decrease is related to the removal of the extractable fraction of PNS [16,38]. Conversely, the peaks at 1730 and 1281 cm^{-1} showed a slight increase. These signals are related to the C=O stretching vibrations of the acetyl moieties and C-H deformation of the holocellulose fraction of NS, respectively [12,17], and were comparatively higher in NS1 because of the removal of the ethanol extractable matter.

The effect of ball-milling on the biomass was followed by FTIR analysis (full IR spectra are reported in Fig. S2b in SI). After ball-milling, the spectra showed several changes with the treatment time (Fig. 1). In the carbonyl region, the intensity of the C=O stretching signal at 1730 cm^{-1} (Fig. 1a), as well as that at 1029 cm^{-1} (Fig. 1d), ascribed to secondary alcohols, aliphatic

Eliminato: Eliminato: [19].

Eliminato: PNS was first treated with ethanol to recover valuable low molecular weight polyphenolic substances that can be used as functional additives in polymer compounding and other formulations [18,35]. Among alcohols, ethanol is considered an economically viable and environmentally safe solvent. It is used to extract substances with a low molecular weight such as phenolic compounds [35–37], and was recently recommended as a green solvent in oil extraction [38,39]. ¶

The FTIR spectrum of the biomass after extraction (NS1) is reported in Fig. S2a. Compared with the parent NS, an intensity reduction in the hydroxyl region around 3300 cm^{-1} was noticed. Similarly, a remarkable intensity decrease wasdetected for the signals correlated to the C–H stretching vibrations of methylene (2923 cm^{-1}) and methyl groups (2855 cm^{-1}). This decrease is related to the removal of the extractable fraction of PNS [17,40]. Conversely, the peaks at 1730 and 1281 cm^{-1} showed a slight increase. These signals are related to the C=O stretching vibrations of the acetyl moieties and C-H deformation of the holocellulose fraction of NS, respectively [18,19], and were comparatively higher in NS1 because of the removal of the ethanol extractable matter. ¶ The effect of ball milling on the biomass was followed by FTIR analysis (full IR spectra are reported in Fig. S2b in SI). After ball milling, the spectra showed several changes with the treatment time (Fig. 1). In addition, the intensity of the C=O stretching signal at 1730 cm^{-1} (Fig. 1a), as well as that at 1029 cm^{-1} (Fig. 1d), ascribed to secondary alcohols, aliphatic ethers, or to β-(1→4) linkages [41], increased remarkably. On the other hand, the absorption at 1190 cm^{-1} due to the pyranose ring C-O bonds [42] abruptly decreased (Fig. 1c). This evidence indicates that the mechanochemical treatment favored the cleavage of the polysaccharide fraction from the lignocellulosic biomass as well as the occurrence of oxidation reactions. Other changes were noticed in the aromatic skeletal vibration (1604 cm^{-1}) and fingerprint regions of the spectrum (Fig. S2b). In particular, a strong decrease in the absorption peaks at 1280 cm^{-1} (Fig. S2 b) accounted for the amorphization of the cellulose fraction, as also reported for ball milled spruce wood and cotton cellulose [43,44].¶

ethers, or β-(1→4) linkages [39], increased remarkably. On the other hand, the absorption at 1190 cm^{-1} due to the pyranose ring C-O bonds [40] abruptly decreased (Fig. 1c). This evidence indicates that the mechanochemical treatment favored the cleavage of the polysaccharide fraction from the lignocellulosic biomass as well as the occurrence of oxidation reactions. Other changes were noticed in the aromatic skeletal vibration (1604 cm^{-1}) and fingerprint regions of the spectrum (Fig. S2b). In particular, a strong decrease in the absorption peaks at 1280 cm^{-1} (Fig. 1 b) accounted for the amorphization of the cellulose fraction, as also reported for ball-milled spruce wood and cotton cellulose [41,42].

3.1.2. Morphological and size characterization

Figure 2 shows the SEM images of the biomass before and after 30 minutes of milling. Neat NS1 exhibited two main morphologies, consisting of elongated structures and irregularly shaped particles. A more detailed view of the former revealed the complex fibrous structure of wellpreserved vascular bundles, consisting of an arrangement of parallelly aligned spiral cellulose microfibrils embedded in a thin cohesive matrix made of lignin and hemicellulose [12]. After 30 minutes of treatment (NS2) there was almost no trace of the fibrillar and spiral-arranged fractions, and only irregularly shaped particles were visible, with dimensions ranging from 1 to 10 µm. This outcome paralleled the disappearance of the peak at 1280 cm^{-1} (Fig. 1b) in the milled samples as a result of the reduction of the crystalline structures by ball-milling [12,38,40,42]. Higher magnification images showed that the length of the fibrils of pristine biomass dropped to a few microns, and the smaller particles tended to agglomerate (Fig. S3). This was probably caused by the complex structure of lignocellulose and the higher surface energy associated with size reduction. By increasing the ball-milling time to 120 min, the shape and dimensions of the particles remained almost unchanged [43]. This last observation could be attributed to strong hydrogen bonding and van der Waals forces in the complex structure of the biomass [44].

To get further insight on the effect of ball-milling on the size distribution, the biomass was characterized by Dynamic Light Scattering (DLS). Fig. S4 shows the DLS curves at different milling extents. Before ball-milling, the average size of the biomass was well above the instrumental detection limit (10 µm).

Therefore, no measurement could be recorded for NS1. A 30 minute milling dramatically reduced the average size of the biomass, as a distribution peak of 2.7±0.2 μm was determined for NS2. Increasing the ball-milling time to 120 minutes resulted in a further decrease in size, down to 1.5±0.2 μm for NS4.

Eliminato: morphological arrangements

Eliminato: parallel **Eliminato:** [19].

Eliminato: μm

Eliminato: , were visible

Eliminato: 1b) in the milled samples as a result of the reduction of the crystalline structures by ball milling [19,40,42,44]. Higher magnification images showed that the length of the fibrils of pristine biomass dropped to a few microns, and the smaller particles tended to agglomerate (Fig. S3). This was probably caused by the complex structure of lignocellulose and the higher surface energy associated with size reduction. By increasing the ball milling time to 120 min, the shape and dimensions of the particles remained almost unchanged [45]. This last observation could be attributed to strong hydrogen bonding and van der Waals forces in the complex structure of the biomass [46]

Eliminato:

Eliminato: onsize

Spostato (inserimento)

[1] Eliminato: Figure

Eliminato: size distribution

Eliminato:

Eliminato:),

Eliminato: size distribution

Eliminato:

Eliminato: 60 and

Eliminato: brought

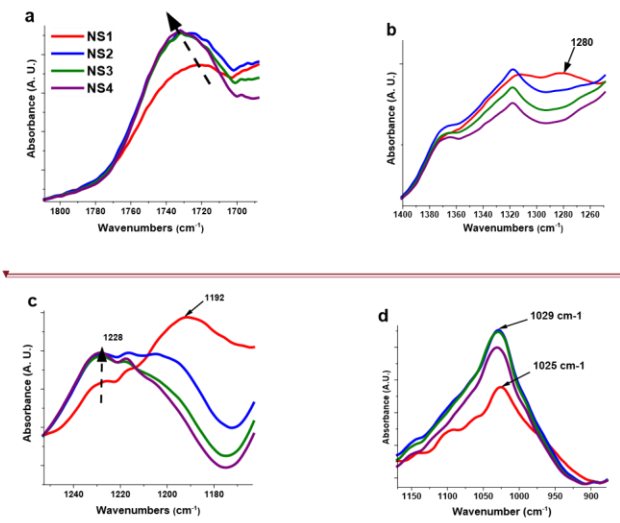

Figure 1. Evolution of FTIR spectra relative to ball-milled biomass at different treatment times. This picture reports the regions where major changes are detected. Full spectra are shown in Fig. S2.

Eliminato: ¶

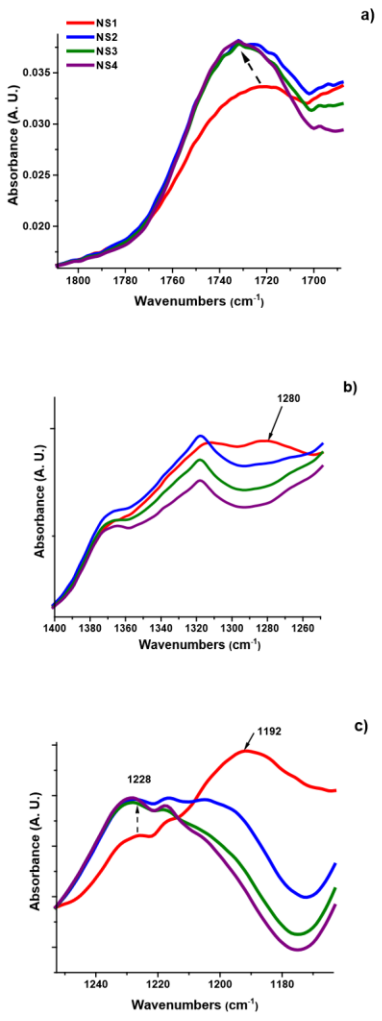

...

Eliminato:

Eliminato: Figure

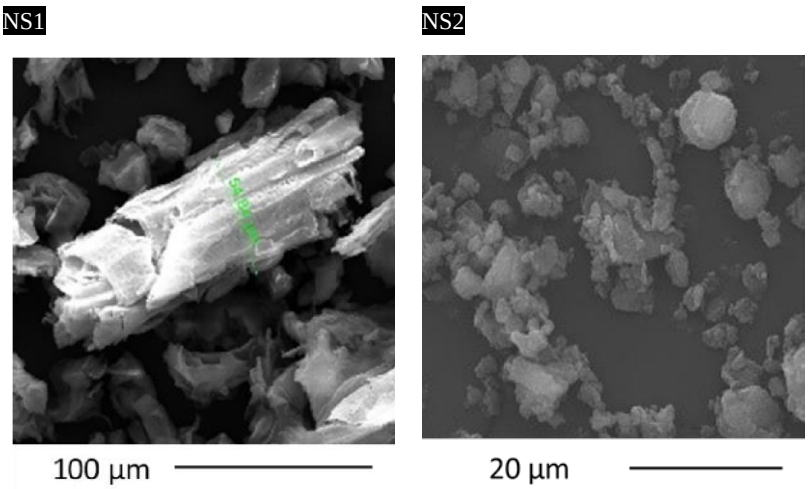

Figure 2. SEM images of NS1 (unmilled) and NS2 (30 min ball-milling).

3.1.3. Thermal analysis

TGA was carried out on PNS derivatives to assess any changes in filler degradation temperature with ball-milling time. TGA curves in nitrogen and the corresponding DTG plots are reported in Fig. S5a in the SI. TGA analyses in air were also carried out (Fig. S5b). In this case, the curves demonstrated an unpredictable behavior at the end of the measurement due to the rapid combustion of the residual char under a 10 ºC min^{-1} heating rate. Therefore, an additional measurement under air atmosphere at 1 ºC $min^{-1}$was performed (Fig. S5c). The corresponding parameters under air are reported in Table S1.

The main TGA parameters are reported in Table 2. Compared with NS1, ball-milling did not affect the shape of the degradation curves, and the mechanochemical treatment scarcely affected the T_{onset} values. T_{max1} showed some change but remained approximately in the value range of the non-ball milled biomass. T_{max2} displayed a decreasing trend with ball-milling time, likely due to the amorphization of the cellulose component. On the contrary, slightly higher residual char values were noticed for the ball-milled samples, as the mechanochemical treatment promoted the dehydration of the biomass, which favored charring. Similar behaviors were reported by Ling et al. [41] on ball-milled cotton, as well as Kim et al. [45] that carried out a TGA study on cotton, tunicate cellulose, and microcrystalline cellulose.

Table 2. TGA data under nitrogen of PNS derivatives at different times of milling (heating rate 10 ºC min^{-1}).

Sample	Nitrogen	
	T_{onset} (ºC)	T_{max} (ºC)
NS1	245.6	I) 297.1 II) 363.7
NS2	245.9	I) 290.5 II) 360.3
NS3	249.3	I) 295.7 II) 349.2
NS4	245.8	I) 295.4 II) 349.1

Eliminato:

Eliminato: **Eliminato:**

and structural

Eliminato:

Eliminato: , along with

Eliminato: , obtained in nitrogen atmosphere,

Eliminato: Figure

Eliminato:),

Eliminato: however,

Spostato (inserimento) [2]

Eliminato: As shown in

Spostato in su [1]: Fig.

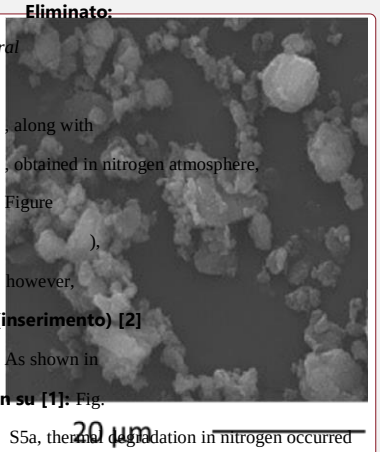

Eliminato: S5a, thermal degradation in nitrogen occurred via a multi-step process, consistent with the complex

...

Spostato in su [2]: The main TGA parameters are reported in Table 2.

Eliminato: ¶

Compared with NS1, ball milling did not affect the shape of

...

Eliminato:

Eliminato:

Formattato: Tipo di carattere: Non Corsivo **Eliminato:** [43]

Formattato: Tipo di carattere: Non Corsivo

Eliminato: [47] that carried out a TGA study on cotton, tunicate cellulose and microcrystalline cellulose.

*at 600ºC. I, and II refer to the first, and second thermo-degradative steps.

3.2. Characterization of PLA biocomposites

3.2.1 Rheology and MFR

The viscoelastic response of pure PLA and PLA biocomposites was investigated to evaluate the effect of the fillers on PLA melt rheology. Dynamic frequency sweep (DFS) tests showed that the polymer melt behavior was mainly viscous (G′<G″) for all samples, and both moduli approached constant values in the rubbery plateau region above 100 rad s^{-1}, where moduli crossover occurred (Figure 3a). The addition of PNS derivatives significantly enhanced the viscoelastic response of PLA, as G′ and G″ values of the biocomposites exceeded those of PLA over the entire frequency range investigated. PN1 exhibited the highest moduli, while the other biocomposites displayed a slight reduction. A plateau in G′ was observed at low frequency for the biocomposites, particularly for PN3 and PN4, indicating the transition from liquid-like to solid-like viscoelastic behavior, which was more marked for the biocomposites containing filler with a smaller size distribution. The complex viscosity curve of pure PLA (Fig. 3b) showed a shear thinning behavior for frequency values higher than 10 rad s^{-1}, and a Newtonian plateau at low frequencies [12]. On the other hand, at low frequency, the biocomposites viscosity curves turned up from the Newtonian plateau. This result can be explained in terms of the formation of a three-dimensional interconnected particulate network in the melt, as well as the restricted mobility of the polymer melt due to the interaction between the polymer chains and filler particles [12,16,17]. Furthermore, PN1 presented the highest complex viscosity, which slightly decreased in the biocomposites charged with the ball-milled biomass, highlighting the importance of the lower size and the shape of the filler after the mechanochemical treatment [46,47].

To gain further insight on this effect, MFR of PLA and PLA-based biocomposites were also measured (Fig. 3c). Melt flow rate values provide information on the processability of the polymeric material through injection molding, extrusion, thermoforming or printing [48]. In polymer composites, MFR values are affected by the load and shape of the filler [20,32] as well as by its interaction with the matrix [19]. In addition, the friction between filler and matrix affects the melt flow. As expected, the presence of filler significantly reduced the MFR value of PN1 (0.55 g min^{-1}) compared to plain PLA (0.85 g min^{-1}), as the interparticle interactions significantly restricted the relative motion between macromolecules [32,49]. Very interestingly, increasing the ball-milling time allowed to recover the melt fluidity. A similar behavior was reported by Gallagher et al. [18], since the reduction of the particle size of wood fiber in maleated polyethylene composites increased the MFR value. Likewise, in biocarbon-filled poly(trimethylene terephthalate) (PTT)/PLA blend composites, the size reduction of the filler particles dramatically reduced the shear viscosity of the composites, which dropped below that of the matrix [49]. The main reasons for the particle size-related decrease in viscosity are the dilution of the polymer chain entanglement density, the selective interaction of polymer chains on the particle surface, and the lower resistance against shear stress [21,49]. Notably, in terms of polymer processability, ballmilling of NS1 made polymer flow and forming procedures easier, hence lowering the energy requirements for manufacturing [50].

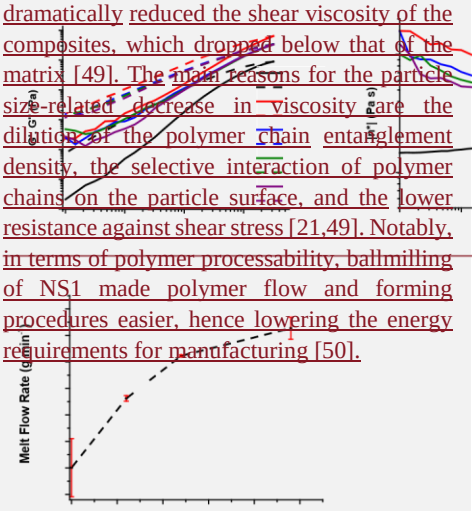

Eliminato: PN1 exhibited the highest moduli, while

Eliminato: the other biocomposites displayed a slight reduction. A plateau in G′ was observed at low frequency for the biocomposites, in particular for PN3 and PN4, indicating the transition from liquid-like to solid-like viscoelastic behavior, which was more marked for the biocomposites containing filler with a smaller size distribution. The complex viscosity curve of pure PLA (Figure 3b), showed a shear thinning behavior for frequency values higher than 10 rad s^{-1}, and a Newtonian plateau at low frequencies [19]. On the other hand, at low frequency, the biocomposites' viscosity curves turned up from the Newtonian plateau. This result can be explained in terms of the formation of a three-dimensional interconnected particulate network in the melt, as well as the restricted mobility of the polymer melt due to the interaction between the polymer chains and filler particles. These results are consistent with those reported by other authors in similar systems [17–19]. Furthermore, PN1 presented the highest complex viscosity, which slightly decreased in the biocomposites charged with the ball milled biomass, highlighting the importance of the lower size and the shape of the filler after the mechanochemical treatment [48,49]. ¶ To gain further insight on this effect, MFR of PLA and PLAbased biocomposites were also measured (Fig. 3c). Melt flow rate values provide information on the processability of the polymeric material and its destination to injection molding, extrusion, thermoforming or printing [50]. In polymer composites, MFR values are affected by the load and shape of the filler [22,34] as well as by its interaction with the matrix [21]. In addition, the friction between filler and matrix affects the melt flow. As expected, the presence of filler significantly reduced the MFR value of PN1 (0.55 g min^{-1}) compared to plain PLA (0.85 g min^{-1}), as the interparticle interactions significantly restricted the relative motion between macromolecules [34,51]. Very interestingly, increasing the ball milling time allowed the recovery of the melt fluidity. A similar behavior was reported by Gallagher *et al*. [20], where the reduction of the particle size of wood fiber into maleated polyethylene composites increased the MFR value. Likewise, in biocarbon-filled poly(trimethylene terephthalate) (PTT)/poly(lactic acid) (PLA) blend composites, the size reduction of the filler particles dramatically reduced the shear viscosity of the composites, which dropped below that of the matrix [51]. The main reasons for the particle size-related decrease in viscosity are the dilution of the polymer chain entanglement density, selective interaction of polymer chains on the particle surface, and lower resistance against shear stress [23,51]. In terms of polymer processability, ball milling of NS1 made polymer flow and forming procedures easier, hence lowering the energy requirements for manufacturing ...

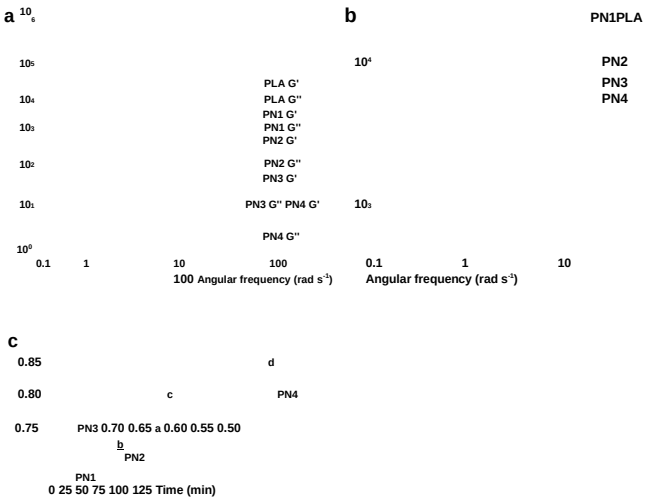

Figure 3. Rheological characterization of PLA and its biocomposites. a) storage and loss moduli (G' and G'', respectively); b) complex viscosity (η^*) vs the angular frequency. c) Relation between Melt flow rate and ball-milling time.

3.2.2. Thermal characterization

The thermal stability of PLA and the prepared biocomposites was assessed by TGA. Thermogravimetric curves obtained under nitrogen are reported in Fig. S6a. Both PLA and its biocomposites exhibited a single-step weight loss process. Neat PLA was characterized by a fast weight drop stage with nearly no char residue. The biocomposites showed a slower degradation process with a residual weight at 600 °C close to 24 wt.% that was independent of the filler ball-milling duration. Thermogravimetric parameters are reported in Table 3. The T_{onset} of neat PLA was 268.1 °C. Compared to the neat matrix, all biocomposites exhibited higher T_{onset}, especially those containing the ball-milled biomass, with values ranging from 269 °C to 277 °C. As for the temperature of maximum decomposition rate, PLA showed a T_{max} of 304 °C, which increased by nearly 10 °C for PN1 and reached a maximum for PN3 (328.3 °C). The T_{max} improvement of biocomposites can be attributed to a slow thermal degradation rate of the biomass. The effect is more remarkable for samples charged with ball-milled filler due to the finer dispersion of the latter [44]. Summing up, the presence of the biomass increased the thermal stability in inert atmosphere. In particular, the milling treatment of the filler enhanced the T_{max} values (PN3).

TGA measurements were also carried out in air (Fig. S6b). Table S1 in the SI summarizes the calculated thermal parameters. Under air, the higher stability of the biomass contributed to an increase in the T_{max} values of the biocomposites with respect to PLA. The curves and a more detailed discussion are reported in the SI.

Table 3. TGA data of PLA and its biocomposites under nitrogen.

	T_{onset} (°C)	T_{max} (°C)	Char. Yield (% wt.)*
PLA	268.1	304.2	2.7
PN1	277.4	312.9	21.6
PN2	269.8	325.8	25.1
PN3	274.7	328.3	24.6
PN4	268.7		

Eliminato:

Spostato in giù [3]: TGA measurements were also carried out in air (Fig.

Eliminato: S6 b

Spostato in giù [4]:). Table S1 in the SI summarizes the calculated thermal parameters.

Eliminato: Figure

Eliminato: In nitrogen, both **Eliminato:** (Fig. S6a).

Eliminato:

319.0 21.4

*at 600ºC.

DSC characterization of PLA and its biocomposites was carried out on the compression molded and annealed samples. Curves related to the first heating scan are shown in Fig. 4 as they are more informative concerning the effects of processing on the properties of the material. All curves showed a change in heat capacity at about 60 °C due to the glass transition, an exothermic peak at around 100 °C due to cold crystallization, and finally the melting endotherm. The latter always appeared as a complex signal featuring two components, related to α'- (147 ºC) and α- (153 ºC) forms, as reported by Cocca et al. [28]. The thermal parameters relative to the DSC traces are listed in Table 4. The T_g was not affected by filler or ball-milling. As for the cold crystallization, PLA exhibited a T_c of 110 °C and a crystallization enthalpy (ΔH_c) equal to 23.6 J g^{-1}. Compared to the plain polyester, all the studied biocomposites showed a shift towards lower temperatures of T_c, that was independent of ball-milling treatment. Regarding the ΔH_c values, PN1 composite (based on non-treated biomass) did not show any change of the parameter. Conversely, biocomposites filled with ball-milled biomass revealed a not negligible improvement of this property. The effect was particularly notable in the PN3 sample (60-min ball-milling) with a ΔH_c value increase of

Eliminato: time of the filler.

Eliminato: of the investigated samples

Eliminato: the studied **Eliminato:** the samples

Eliminato:

Eliminato: this value **Eliminato:** and to its charring capability.

Eliminato:

Spostato (inserimento) [3]

Spostato (inserimento) [4]

Eliminato: [46]. Summing up, the presence of the biomass increased the thermal stability in inert atmosphere; in particular, the milling treatment of the filler enhanced the T_{max} values (PN3). As far as TGA curves under air atmosphere are concerned

Formattato: Posizione: Orizzontale: Al centro, Rispetto a: Colonna

Tabella formattata

Formattato: Posizione: Orizzontale: Al centro, Rispetto a: Colonna

Formattato: Posizione: Orizzontale: Al centro, Rispetto a: Colonna

Formattato: Posizione: Orizzontale: Al centro, Rispetto a: Colonna

Formattato: Posizione: Orizzontale: Al centro, Rispetto a: Colonna

Formattato: Posizione: Orizzontale: Al centro, Rispetto a: Colonna

Formattato: Posizione: Orizzontale: Al centro, Rispetto a: Colonna

Formattato: Posizione: Orizzontale: Al centro, Rispetto a: Colonna

Eliminato: DSC curves of PLA and the biocomposites (compression moulded samples) are reported in Fig. 4. As the first heating scan (Fig. 4a) is more informative concerning the effects of processing on the properties of the material, the analysis of the calorimetric data was carried out on the first DSC run. All the studied specimens first showed a change in heat capacity at about 60 °C, relative to the glass transition, followed by an exothermic peak centered around 100 °C, due to a cold crystallization phenomenon, and finally the melting endotherm. The latter always appeared as a complex signal featuring two components, related to α'- (147 ºC) and α- (153 ºC) forms, as reported by Cocca et al. [30]. The thermal parameters relative to the DSC traces are shown in Table 4. Compared to neat PLA, the T_g was scarcely affected by the ...

about 24%, Summarizing, the filler decreased the temperature of cold crystallization, and its nucleating action was more remarkable after ball-milling. Nucleating effects of biobased fillers have been previously reported for PLA/Sisal fibre composites [51], PLA/pecan nutshell [16,17] and other polymeric systems ~~charged with natural fibers [52–54].~~

The mechanochemical treatment of the filler also affected the melting properties of the biocomposites. As shown in Table 4, the presence of the filler did not affect the T_m relative to the double melting phenomenon but influenced their relative intensity. Furthermore, the total enthalpy of melting (ΔH_m) followed the same trend recorded for ΔH_c. Indeed, PN1 showed the same ΔH_m value as neat PLA (25 J g^{-1}), while biocomposites charged with ball-milled fillers exhibited an improvement in total melting enthalpy. This confirmed the more remarkable nucleating action of the ball-milled biomass. Notably, all the ΔH_m values were slightly higher than the corresponding ΔH_c, indicating that the compression molded samples partly crystallized during cooling. DSC traces relative to the second heating are displayed in Fig. S7a in the SI, and their thermal parameters are shown in Table S2. All the reported curves showed the same experimental features

discussed for the first heating run. The same can be said for the values of the experimental parameters.

Among post processing methods established for optimizing the structure and morphology of polymer-based materials, thermal annealing has been commonly used, becoming even indispensable for improving the final product or device performance [5,55]. In the following experiments, the samples were subject to annealing at 75 ºC to improve thermal and mechanical properties of the biocomposites. Fig. 4b displays the first heating DSC curves of PLA and biocomposites after annealing, while the corresponding calorimetric data are reported in Table 4. Remarkably, after the thermal treatment no signal related to the glass transition was noticed, except for PLA, which displayed a T_g increase of about 4 °C compared to the non-annealed counterpart. Besides, none of the samples showed any crystallization exothermal peak, indicating that thermal annealing caused the samples to crystallize. Finally, most of the investigated samples exhibited a single melting endotherm, or possibly a barely visible shoulder on the low temperature side of the peak. In this respect, T_m values were scarcely influenced by sample composition, and fell roughly in between the values of the two melting peaks recorded before annealing. The associated ΔH_m values showed some remarkable effects attributable to the thermal treatment, the presence of the filler and the ball-milling duration. ~~PLA exhibited a ΔH_m equal to 28.8 J g^{-1}, which increased to~~ 32.5 J g^{-1} for PN1, containing the untreated filler. A more remarkable increase of ΔH_m was recorded when the biomass was submitted to ball-milling. The maximum effect was observed after 30 minutes of treatment (sample PN2, 39.5 J g^{-1}), slightly decreasing at higher times. The reported results evidenced the effectiveness of thermal annealing in the morphological stabilization of PLAbased products. In addition, they confirm the role of the biomass as a nucleating agent towards PLA matrix and suggest that ball-milling can significantly improve its action. Finally, the degree of crystallinity (χ_c) was calculated for all samples. Before annealing, PN1 showed a crystallinity similar to neat PLA, while in ball-milled biocomposites this parameter increased at longer milling time. The same behavior was also observed in the samples after annealing.

Eliminato: [6,57]. In this experiment, annealing at 75 ºC was applied to the prepared samples in order to analyze the effects of thermal treatment on mechanical and physical properties of the pecan biomass reinforced biocomposites.

Eliminato: ,

Eliminato: for

Eliminato: the

Eliminato: increased by

Eliminato: with respect

Eliminato: its

Eliminato:

Eliminato: processing that was used.

Eliminato: this value

Eliminato:

Eliminato: evidence

Eliminato:

Commentato [CN3]: I suggested an alternative to "remarkably" because the word "remarkably" is used quite frequently throughout the text.

Eliminato:

Eliminato:

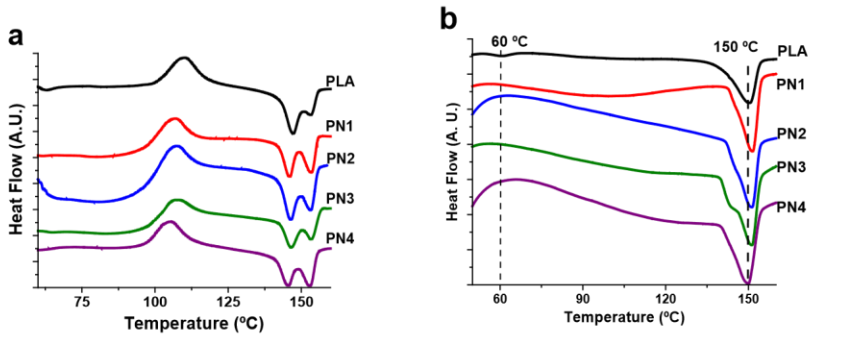

Figure 4. DSC curves (first heating scan) of PLA and its biocomposites, a) before and b) after thermal annealing (at 75 ºC for 72 h).

Table 4. Thermal parameters measured by DSC (first heating scan, 5 °C min^{-1}), for PLA and i biocomposites.

Sample	Before annealing							After annealing[a]			
	T_g (ºC)	T_c (°C)	ΔH_c (J g^{-1})	T_m (ºC)	ΔH_m **[b] (J g^{-1})	ΔH_m *[c] (J g^{-1})	χ_c (%)	T_g (ºC)	T_m (ºC)	ΔH_m (J g^{-1})	χ_c (%)
PLA	58.8	110.2	23.6	147.0 153.0	21.5 3.4	24.9	20.1 2.4	62.8	150.5	28.8	23.0
PN1	57.4	106.7	23.7	146.1 153.3	17.4 7.6	25.0	16.2 5.3	-	151.53	32.5	26.0
PN2	61.4	106.7	25.4	146.5 153.0	19.4 6.7	26.0	18.1 4.7	-	151.2	39.5	31.6
PN3	61.5	105.0	29.2	146.8 153.5	23.6 6.3	29.9	22.1 4.4	-	151.3	36.8	29.4
PN4	58.7	105.4	28.7	146.8 153.1	21.4 8.2	29.6	20.0 5.7	-	150	35.1	28.0

[a]performed at 75 ºC for 72 h. [b]the respective contribution of the two melting peaks (related to α'- and forms) was calculated. [c]corresponds to the sum of the two peaks.

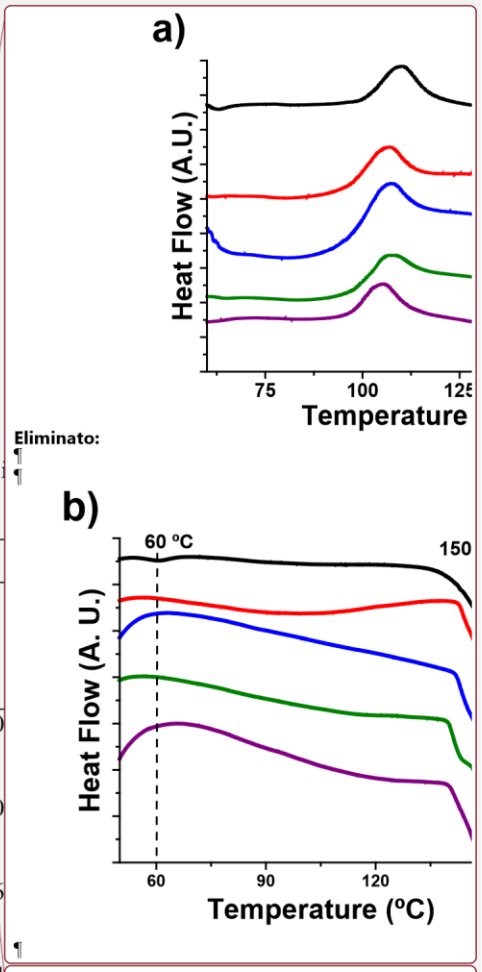

Eliminato: ¶ ¶

Tabella formattata

Eliminato: annealing*

Eliminato: ***

Eliminato: *

Eliminato: **the

Eliminato: ***corresponds

Eliminato: both detected

The effect of thermal annealing on the structure of the investigated samples was further studied by FTIR spectroscopy. The development of crystallinity was assessed by monitoring the absorption band at 923 cm^{-1}, characteristic of the ordered crystalline phase of PLA [56] and attributed to the combination of C–C backbone and CH_3 rocking mode of α crystals [29,57]. Fig. 5a shows the analytical peak upon increasing annealing times for neat PLA. It was noticed that this signal was completely absent before annealing, and progressively rose with the treatment time. Furthermore, the evolution of the signal was fast in the first few hours of treatment and slowed down at longer times. Similar results were obtained for all the biocomposites, as reported for PN1 in Fig. S8 in the SI. The conversion from the amorphous to the crystalline form was quantitatively followed by analyzing the ratio of the integrated absorbance of the peaks at 923 cm^{-1} and 950 cm^{-1} (A_{923}/A_{950}), the latter arising from the amorphous fraction of PLA [29]. The absorbance ratios of the studied samples are reported in Fig. 5b as a function of the annealing time. In all cases most of the crystallization process occurred during the first 24 hours of thermal treatment while after 72 hours a plateau was reached. The latter outcome evidences that at this annealing time, the crystallization process is almost complete, and samples used for bulk characterization were fully crystallized. It was noticed that at low annealing times PN1 exhibited higher conversion rates than PLA. Furthermore, all biocomposites, compared to the neat matrix, reached larger plateau values of the parameter at longer times. This evidence agrees with DSC results, which showed higher crystallinity degrees for composites and further confirmed the nucleating action of the filler towards the thermoplastic matrix. However, no differences in biocomposites crystallinity were noticed by FTIR analysis after the thermal annealing.

Eliminato: ¶

Eliminato: The analysis was carried out on neat PLA as well as on the biocomposites.

Eliminato: [58]

Eliminato: [31,59].

Eliminato: prior to

Eliminato: is

Eliminato: slows

Eliminato: can be

Eliminato: , in a more quantitative way,

Eliminato: [31].

Eliminato: The data evidenced that in

Eliminato: were noticed on the attained

Eliminato: due to

Eliminato: post treatment among biocomposites by FTIR analysis

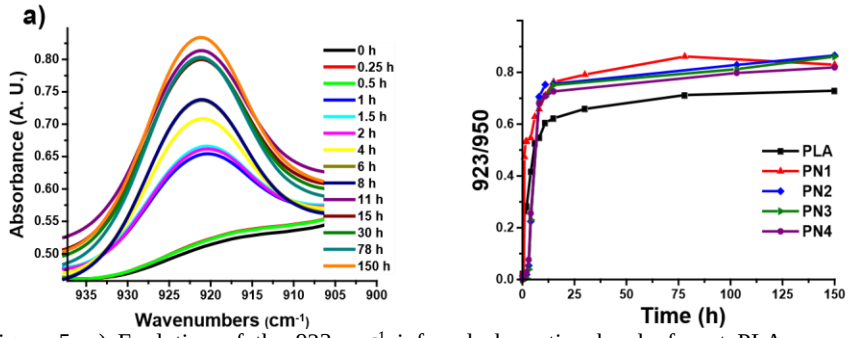

Figure 5. a) Evolution of the 923 cm^{-1} infrared absorption band of neat PLA upon time. b) Conversion progress from amorphous to crystalline form due to annealing followed by A_{923}/A_{950} ratio as a function of the annealing time for PLA and its biocomposites.

3.2.3. Thermomechanical properties

One of the possible applications of biodegradable polymers is to replace their conventional counterparts for manufacturing disposable plates and cups, which come in contact with hot food or beverages. In this respect, PLA exhibits poor resistance to high temperature and low HDT, that is a measure of the ability of the polymer to bear a given load as a function of temperature. The HDT value of a polymeric material depends on stiffness and glass transition temperature. In addition, in polymer composites, it can be also influenced by filler size distribution, aspect ratio and filler content. Therefore, in the present paper, HDT measurements were carried out to assess the possible influence of filler milling and thermal annealing on this parameter.

The deflection versus temperature plots of the prepared samples before and after annealing are reported in Fig. 6. It is noticed that the prepared biocomposites showed higher deformability with the temperature when compared with plain PLA. This finding is

confirmed by the HDT values [58] reported in Table 5. This decay could be due to the presence of filler particles that increase the number of defects at the charge-matrix interface. Moreover, ball-milling of the biomass resulted in further decreased HDT values, likely due to the low aspect ratio of the particles. However, since the PNS derivatives demonstrated to be effective nucleating agents, able to increase PLA crystallinity and in turn to improve its thermomechanical performance, HDT measurements were carried out also on thermally annealed samples.

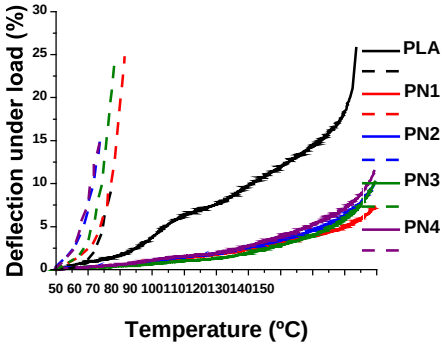

Figure 6. Deflection under load versus temperature for PLA and its biocomposites. Dashed lines: samples before annealing. Solid lines: samples after annealing (at 75 ºC for 72 h).

Table 5. HDT parameters calculated for PLA and its biocomposites.

Sample	Before HDT (°C)	After annealing* HDT(°C)	Strain at 140 ºC (%)
PLA	63.1	77.1	18.5
PN1	61.0	118.5	5.0
PN2	56.7	114.9	6.3
PN3	59.9	121.6	5.9
PN4	56.2	112.6	7.1

*at 75 ºC for 72 h.

All the annealed samples showed a significant decrease in deformability with respect to the pristine ones, and the effect was dramatically enhanced for the biocomposites. This outcome is even more detectable if the values of strain at 140 °C are considered (Table 5). The value of this parameter was 18.5 % for neat PLA and dropped to 5-7 % in the composite samples. In the same table, HDT values are also reported. By comparing the HDT data of pristine and heat-treated samples, an outstanding improvement of the parameter was noticed. Even in this case, the effect was more remarkable for the biocomposites. Annealed PLA showed a HDT value of 77 °C, with a 14 °C increase with respect the pristine sample. Biocomposites exhibited HDT values ranging from 113 °C to 121 °C, with as nearly as 60 °C improvement compared to the non-annealed samples. This result highlighted the dramatic impact of crystallinity, as measured by DSC and FTIR spectroscopy, on the thermomechanical properties of PLA. The effects of filler loading and annealing on HDT have been reported for PLA [59], PLA blends [55], and composites filled with natural fibers

Eliminato: [60] reported in Table 5.

Eliminato:

Eliminato: correspond to curves samples

Eliminato: , solid

Eliminato: refer to annealed

and mineral fillers [51,60,61,62]. As for the thermomechanical behavior of nonannealed PLA composites, most authors report that the presence of the charge scarcely influence HDT values which remains in the range of the plain matrix [51,60], in agreement with our results. However, after annealing, an improvement of thermomechanical performance is often recorded.
The effect is detected either on neat PLA and its compounds but is more remarkable for composites [51,60–62] due to the nucleating action of the filler towards the matrix. The development of transcrystallinity at polymer-matrix interface during annealing can have a role in HDT improvement [51], however, filler dimensions can also affect the HDT performances of the materials [62].

3.2.4. SEM analysis of cryofractured surfaces

SEM analysis of the cryogenically fractured surfaces of the PLA and PLA biocomposite plates provided insight on filler distribution and morphological properties of the samples, as well as on the interfacial adhesion between filler and matrix. Micrographs relative to PLA, PN1 and PN2, before and after annealing, are reported in Fig. 7. The corresponding images related to PN3 and PN4 are reported in the SI (Fig. S9). As for non-annealed samples, PLA showed a fracture surface almost featureless typical of glassy polymeric materials. The investigated biocomposites exhibited

Eliminato: ¶

¶

All the annealed samples showed a significant decrease in deformability with respect to the pristine ones, and the effect was dramatically enhanced for the biocomposites. This outcome is even more detectable if the values of strain at 140 °C are considered (Table 5). The value of this parameter was 18.5 % for neat PLA and dropped to 5-7 % in the composite samples. In the same table, HDT values are also reported. By comparing the HDT data of pristine and heat-treated samples, an outstanding improvement of the parameter was noticed. Even in this case, the effect was more remarkable for the biocomposites. Annealed PLA showed a HDT value of 77 °C, with a 14 °C increase with respect the pristine sample. Biocomposites exhibited HDT values ranging from 113 °C to 121 °C with as nearly as 60 °C improvement compared to the non-annealed samples. This result highlighted the dramatic impact of the crystallinity increase, as measured by DSC and FTIR spectroscopy, on the thermomechanical properties of PLA. The effects of filler loading and annealing on HDT were reported for PLA [61,62], PLA/PCL blends [57], PLA/PMMA blend composites filled with sisal fibers [53], PLA/bamboo fibre/talc hybrid composites [63], PLA loaded with microground paper or talc [64], PLA composites charged with kenaf fibre, nanoclay or hexagonal boron nitride (h-BN) [65]. As for the thermomechanical behavior of nonannealed PLA composites, most authors report that the presence of the charge scarcely influence HDT values which remains in the range of the plain matrix [53,63]. This issue agrees with our results. However, after annealing, an improvement of thermomechanical performance is often recorded. The effect is detected either on neat PLA and its compounds but is more remarkable for composites [53,63–65]. ¶

In agreement with our results, the data in reported literature show that annealing can improve the thermomechanical properties of PLA and that this outcome is magnified in the presence of fillers. Most authors attributed these results to the increase in crystallinity of the system produced by the annealing treatment [53]. The effect was more accentuated for composites due to the nucleating action of the filler towards the matrix. This reasoning is confirmed by the results of Orue *et al*. [53] that recorded HDT values proportional to the filler content and crystallinity. The same explanation was proposed by Shi *et al*. [63]; they also claimed that the development of trans-crystallinity at polymer-matrix interface during annealing can have a role in HDT improvement. However, Wootthikanokkhan *et al*. [65] recognize the importance of crystallinity degree for the thermomechanical properties of polymers and their composites but they also propose that filler dimensions can also affect the HDT performances of the materials. ¶

¶

3.2.4. *SEM analysis of cryofractured surfaces*¶

SEM analysis of the cryogenically fractured surfaces of the PLA and PLA biocomposite plates provided insight on filler distribution and morphological properties of the samples, as well as on the interfacial adhesion between filler and matrix. Micrographs relative to PLA, PN1 and PN2, before and after annealing, are reported in Fig. 7. The corresponding images related to PN3 and PN4 are reported in the SI (Fig. S9). As for …

PLA

a rough and irregularly fractured surface that revealed the inclusion of biomass particles, which appeared to be well dispersed in the polymer matrix. The composite PN1, charged with non-ball-milled biomass, showed the presence of filler particles, with a 15-20 µm dimension range, exhibiting fiber-fracture phenomena. Examination of the matrix-filler interface clearly showed some voids around the particles (delamination), suggesting poor adhesion of the filler to the polymeric phase.

Concerning the effect of the ball-milling, it can be observed that even a 30-minute treatment (PN2 sample) of the biomass resulted in a significantly more homogeneous surface, along with a remarkable reduction of filler domain dimensions with sizes ranging from 15 µm down to 1 µm. It is also noticed that in this case filler fracture was limited to bigger particles , and the prevailing deformation mechanism was fiber pull-out. Longer milling times of the filler did not significantly change the morphology of the fracture surface (PN3 in Fig. S9). The cavities produced by milled PNS particles pull out are clearly visible confirming that the matrix filler interplay between pure PLA and the lignocellulosic filler was not very efficient.

With regards to the fracture surfaces of annealed samples, SEM analysis evidenced that heat treatment scarcely affected the morphology of the studied materials. Compared with the non-annealed specimen, PLA exhibited a rougher surface with a higher number of fracture planes close to each other. The increase in surface roughness was also noticed in the micrographs of the annealed biocomposites and, for PN4 sample (Fig. S9), was so high that the detection of filler particle was no longer possible. Other studies have reported similar effect of the PNS (formation of agglomerates) into PLA, even with lower loadings of filler [16,17].

Not annealed

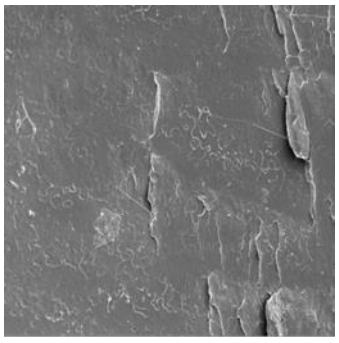

Annealed

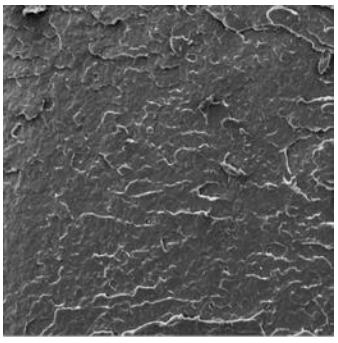

Eliminato:

Eliminato: ,

Eliminato: ,

Codice campo modificato

Eliminato: ,18

Eliminato: Non

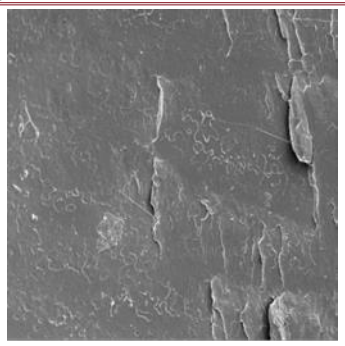

Eliminato:

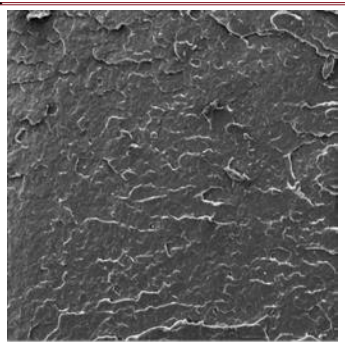

Eliminato:

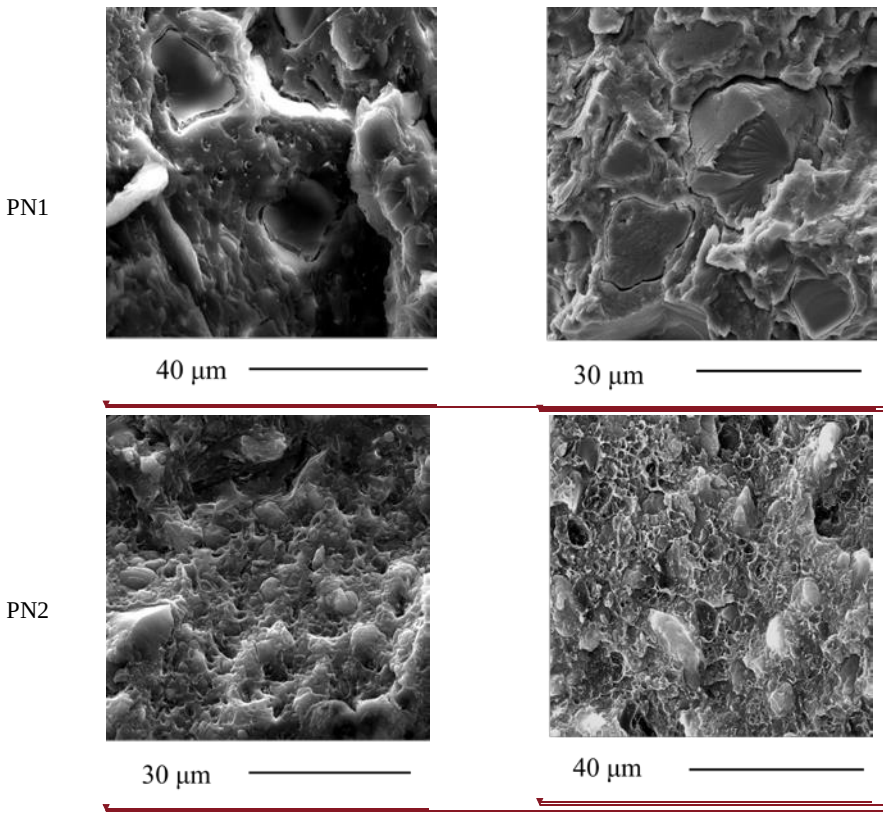

Figure 7. Morphological characterization of PLA and its biocomposites. SEM images of cryofractured surfaces of PLA, PN1, and PN2 before and after annealing (at 75 ºC for 72 h).

3.2.5. Mechanical Properties

The mechanical performance of the pristine and annealed biocomposites was assessed by flexural and impact tests (Table 6). Concerning flexural properties, all the prepared biocomposites showed an enhancement in elastic modulus before annealing with respect to pure PLA. This effect was more significant for PN1, which exhibited a 39% improvement, and less significant for the biocomposites charged with the ball-milled filler. Conversely, the presence of the filler negatively affected the flexural properties of the samples, causing a 30-40 % decrease in stress at break and a more remarkable reduction of strain at break. Impact tests of the investigated biocomposites displayed a drop in toughness with respect to plain PLA. In particular, ball-milling caused resilience to further decrease, attaining less than halved values with respect to the plain polyester. A comparable behavior was noticed for the impact strength, which dropped by about 30% on average. Flexural and impact tests were also performed on samples after annealing. The

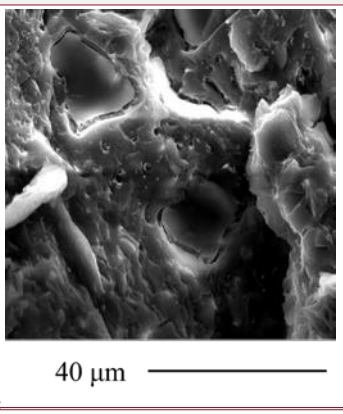

Eliminato:

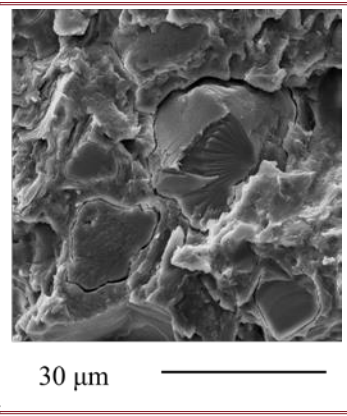

Eliminato:

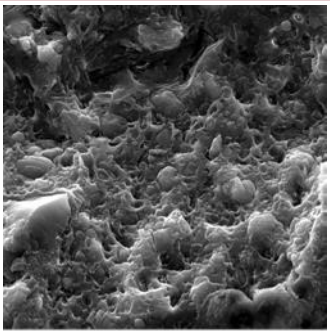

Eliminato:

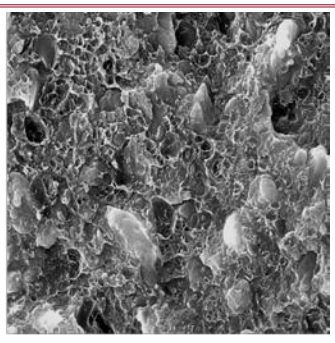

Eliminato:

investigation was carried out on plain PLA and PN1 biocomposite, as the latter was the sample showing the best properties among the prepared samples. Their flexural data reported in Table 6, show that the heat treatment caused an improvement in both modulus and stress at break with respect the corresponding non-annealed samples. The same was observed for the impact strength but not for the resilience values.

The reported results show that pecan nutshell at 50 % loading improves the flexural modulus of the PLA matrix but the stiffening effect is less efficient if the filler if submitted to ball-milling. The flexural data also show that the presence of the filler produces a reduction of stress and strain at break. The latter outcome was also recorded for the impact results that exhibit a decay of both stress and resilience of the biocomposites compared to neat PLA.

The reduced stiffening action of ball-milled fillers can be ascribed to the mechanochemical treatment that brought about amorphization of the cellulosic fraction of the charge, the reduction of molecular weight of its components and the decrease of its aspect ratio [63]. The decay of flexural stress and strain at break and impact properties can be associated to the scarce interaction between the charge and the continuous polymeric phase, as indicated by SEM analysis. Indeed, it has been reported that in polymer composites the ultimate properties are the most sensitive to the filler-matrix adhesion [64].

However, the stiff nature of the fillers employed in this work can also play a role. A similar decay of properties at break has been reported for PLA biocomposites modified with pecan nutshell, oat husk, cocoa shells and apple pomace, as well as in the PBS/Arboform® system [12,16,17,65].

Table 6. Mechanical properties of PLA and its biocomposites.

	FLEXURAL			IMPACT	
	Stress at break (MPa) Before annealing	Modulus (MPa)	Strain at break (%)	Strength (N)	Resilience (KJ/m2)
PLA	82.9±3.7^{d}	3224±291.0^{a}	4.1±0.2^{c}	105.3 ± 5.1^{b}	2.8 ± 0.4^{e}
PN1	55.8±1.5^{b}	4426±166.0^{d,e}	1.3±0.0^{a}	78.3 ± 8.2^{a}	1.2 ± 0.1^{c}
PN2	55.7±0.7^{b}	4337±55.0^{d}	1.3±0.0^{a}	70.5±4.6^{a}	0.9±0.1^{b}
PN3	49.6±0.8^{a}	3937±234.0^{b,c}	1.3±0.1^{a}	61.9±8.4^{a}	0.7±0.1^{a}
PN4	51.2±3.4^{a,b}	4208±159.0^{c,d}	1.2±0.1^{a}	70.3±5.2^{a}	0.8±0.1^{a,b}
After annealing*					
PLA	87.3±8.0^{d}	3631±90.0^{b}	2.8±0.6^{b}	118.0 ± 5.5^{c}	1.9 ± 0.3^{d}
PN1	67.4±7.9^{c}	4691±109.0^{e}	1.5±0.2^{a}	101.5 ± 6.6^{b}	1.1 ± 0.4^{b,c}

^{a}Values with same letter in same column do not present significant difference. *at 75 ºC for 72 h.

Eliminato: [67].

Eliminato: and

Eliminato: as well

Eliminato:

Eliminato: –19,68

Codice campo modificato

Eliminato:

Eliminato: [66].

Eliminato: ¶

As for the effect of annealing on mechanical properties, the improvement of flexural and impact strength data can be associated with the increase of crystallinity produced by the thermal treatment. Similar effects were reported by Chen *et al*. [57] for PLA/PLC blends, and by Li *et al*. [69] on PLA biocomposites reinforced with multi-walled carbon nanotubes. In the latter case, an increase of 9% in strength was obtained after only 2 minutes of thermal annealing at 110 ºC.¶ ¶

As for the effect of annealing on mechanical properties, the improvement of flexural and impact strength data can be associated with the increase of crystallinity produced by the thermal treatment. Similar effects were reported by Chen et al. [55] for PLA/PLC blends, and by Li et al. [66] on PLA biocomposites reinforced with multi-walled carbon nanotubes.

4. Conclusions

In this study, low density, cost-effective, and potentially highly biodegradable

biocomposites have been successfully prepared by charging PLA with a high amount (50 wt %) of pecan nutshell, usually regarded as an agri-food by-product. The effects of ball-milling of the filler and the annealing of the corresponding biocomposites were investigated.

The introduction of the non-ball milled biomass at high loading into the PLA matrix enhanced the polymer viscoelastic response and decreased the MFR. These effects were attributed to the restricted mobility of the polymer melt and the formation of a three-dimensional interconnected particulate network. The presence of the filler also enhanced the polymer thermal stability due to the slower degradation rate of the lignocellulosic biomass with respect to neat PLA. Furthermore, it acted as a heterogeneous nucleating agent, promoting PLA crystallization. It also affected the mechanical properties by improving flexural modulus, reducing flexural stress and strain at break, and impact properties.

Composites charged with ball-milled biomass showed similar features but the effects of the filler on polymer properties were influenced by the mechanochemical treatment applied. Ball-milling of the biomass produced a reduction of particle size along with a deconstruction of the material that involves amorphization, reduction in aspect ratio and mechanical strength. These features affected the properties of the corresponding biocomposites. Indeed, composites based on ball-milled fillers exhibited an increase in MFR and thermal stability, a more pronounced nucleation action, but also a reduction in mechanical properties. Rheological, thermodegradative and morphological effects can be related to the reduction of particle size of the filler while the loss of mechanical properties can be due to its lower mechanical strength.

Finally, thermal annealing increased the mechanical and thermomechanical properties of all materials. In particular, thermal treatment had a dramatic effect the HDT values of the composites that resulted to be on average 50% higher if compared to neat non-annealed PLA.

Overall, these results emphasize the potential of pecan nutshell as a source of sustainable filler to develop cost-effective PLA biocomposites with tailored mechanical properties. These materials could be used when stiff, light, and low deformable products are required, including structural, household, and packaging applications, like food containers, packaging trays, or disposable items.

5. Acknowledgments

Dr. S. Agustin-Salazar thanks to Consejo Nacional de Ciencia y Tecnología (CONACyT- Mexico) for the postdoctoral fellow grant.

Funding from the EU H2020 CE-BG-06-2019 project “Developing and Implementing Sustainability-Based Solutions for Bio-Based Plastic Production and Use to Preserve Land and Sea Environmental Quality in Europe (BIO-PLASTICS EUROPE)” n. 860407, is gratefully acknowledged.

Funding by Regione Lombardia under the ROP ERDF 2014–2020-Axis I-Call Hub Ricerca e Innovazione, project “sPATIALS3” (ID 1176485), is gratefully acknowledged.

6. References

[1] J. Yu, L.X.L. Chen, The Greenhouse Gas Emissions and Fossil Energy Requirement of Bioplastics from Cradle to Gate of a Biomass Refinery, Environ. Sci. Technol. 42 (2008) 6961–6966. https://doi.org/10.1021/es7032235.

[2] O.M. Sanusi, A. Benelfellah, D.N. Bikiaris, N. Aït Hocine, Effect of rigid nanoparticles and preparation techniques on the performances of poly(lactic acid) nanocomposites: A review, Polym. Adv. Technol. 32 (2021) 444–460. https://doi.org/10.1002/pat.5104.

Eliminato: Ball milling

Eliminato: increased

Eliminato: melt flow

Eliminato: corresponding composites. This effect improved

Eliminato: the milling time and can be correlated with the reduction in particle size of the biomass due to the mechanochemical treatment. This outcome can potentially improve the biocomposites processability with techniques such as injection molding, where high fluidity is required. ¶ SEM and

Eliminato: characterization demonstrated that morphology and physical structure of the fillers significantly affected the final properties of the resulting materials. All biocomposites evidenced increased stiffness compared to the plain matrix, and acceptable decrease of

Eliminato: , considering the halved quantity of polymer in the biocomposites

Eliminato: PNS

Eliminato: material

Eliminato: blending

Eliminato: %)

Eliminato:

Eliminato: filler increased the thermal stability of the polymer, and acted as a heterogeneous nucleating agent, increasing PLA crystallinity. This effect was much more evident when thermal annealing was applied to the prepared composites. In particular, after the thermal treatment the HDT values of the composites were an average of 50% higher compared to neat PLA. Rheological properties were also affected, as the **Eliminato:** PNS derivatives

Eliminato: , due

[3] H. Pilz, B. Brandt, R. Fehringer, The impact of plastics on life cycle energy consumption and greenhouse gas emissions in Europe, n.d. https://www.plasticseurope.org/application/files/9015/1310/4686/september-2010-theimpact-of-plastic.pdf.

[4] J. Pimentel, G. Rodríguez, I. Gil, Synthesis of Alternative Cost-Effective Process Flowsheets for Lactic Acid Valorization by Means of the P-Graph Methodology, Ind. Eng. Chem. Res. 59 (2020) 5921–5930. https://doi.org/10.1021/acs.iecr.9b06555.

[5] L. Duan, Y. Zhang, H. Yi, F. Haque, C. Xu, S. Wang, A. Uddin, Thermal annealing dependent dielectric properties and energetic disorder in PffBT4T-2OD based organic solar cells, Mater. Sci. Semicond. Process. 105 (2020) 104750. https://doi.org/10.1016/j.mssp.2019.104750.

[6] H. Cai, V. Dave, R.A. Gross, S.P. McCarthy, Effects of physical aging, crystallinity, and orientation on the enzymatic degradation of poly(lactic acid), J. Polym. Sci. Part B Polym. Phys. 34 (1996) 2701–2708. https://doi.org/10.1002/(SICI)10990488(19961130)34:16<2701::AID-POLB2>3.0.CO;2-S.

[7] K.W. Meereboer, M. Misra, A.K. Mohanty, Review of recent advances in the biodegradability of polyhydroxyalkanoate (PHA) bioplastics and their composites, Green Chem. 22 (2020) 5519–5558. https://doi.org/10.1039/D0GC01647K.

[8] L.-T. Lim, R. Auras, M. Rubino, Processing technologies for poly(lactic acid), Prog. Polym. Sci. 33 (2008) 820–852. https://doi.org/10.1016/j.progpolymsci.2008.05.004.

[9] A. Ahmad, F. Banat, H. Taher, A review on the lactic acid fermentation from low-cost renewable materials: Recent developments and challenges, Environ. Technol. Innov. 20 (2020) 101138. https://doi.org/10.1016/j.eti.2020.101138.

[10] S. Agustin-Salazar, P. Cerruti, G. Scarinzi, 9 Biobased structural additives for polymers, in: Sustain. Polym. Mater., De Gruyter, 2020: pp. 193–234. https://doi.org/10.1515/9783110590586-009.

[11] T. Mukherjee, N. Kao, PLA Based Biopolymer Reinforced with Natural Fibre: A Review, J. Polym. Environ. 19 (2011) 714–725. https://doi.org/10.1007/s10924-011-0320-6.

[12] S. Agustin-Salazar, P. Cerruti, L.Á. Medina-Juárez, G. Scarinzi, M. Malinconico, H. SotoValdez, N. Gamez-Meza, Lignin and holocellulose from pecan nutshell as reinforcing fillers in poly (lactic acid) biocomposites, Int. J. Biol. Macromol. 115 (2018) 727–736. https://doi.org/10.1016/j.ijbiomac.2018.04.120.

Eliminato: [1] C. for I.E.L. CIEL, Fossils, Plastics, & Petrochemical Feedstocks, Fueling Plast. (2017).¶ [2] J.

Eliminato: 3

Eliminato: 4

Eliminato: 5

Eliminato: 6

Eliminato: 7

Eliminato: 8

Eliminato: 9

Eliminato: 10

Eliminato: 11

Eliminato: salazar

Eliminato: 2020.

Eliminato: 12

Eliminato: [13] S. Agustin-Salazar, P. Cerruti, L.Á. Medina-Juárez, G. Scarinzi, M. Malinconico, H. SotoValdez, N. Gamez-Meza, Lignin and holocellulose from pecan nutshell as reinforcing fillers in poly (lactic acid) biocomposites, Int. J. Biol. Macromol. 115 (2018) 727–736. https://doi.org/10.1016/j.ijbiomac.2018.04.120.¶ [14

Spostato (inserimento) [5]

[13] K.L. Pickering, M.G.A. Efendy, T.M. Le, A review of recent developments in natural fibre composites and their mechanical performance, Compos. Part A Appl. Sci. Manuf. 83 (2016) 98–112. https://doi.org/10.1016/j.compositesa.2015.08.038.

[14] L. Berglund, M. Noël, Y. Aitomäki, T. Öman, K. Oksman, Production potential of cellulose nanofibers from industrial residues: Efficiency and nanofiber characteristics, Ind. Crops Prod. 92 (2016) 84–92. https://doi.org/10.1016/j.indcrop.2016.08.003.

[15] A. Bartos, K. Nagy, J. Anggono, Antoni, H. Purwaningsih, J. Móczó, B.

Pukánszky, Biobased PLA/sugarcane bagasse fiber composites: Effect of fiber characteristics and interfacial adhesion on properties, Compos. Part A Appl. Sci. Manuf. 143 (2021) 106273. https://doi.org/10.1016/j.compositesa.2021.106273.

[16] D. Sánchez-Acosta, A. Rodriguez-Uribe, C.R. Álvarez-Chávez, A.K. Mohanty, M. Misra, J. López-Cervantes, T.J. Madera-Santana, Physicochemical Characterization and Evaluation of Pecan Nutshell as Biofiller in a Matrix of Poly(lactic acid), J. Polym. Environ. 27 (2019) 521–532. https://doi.org/10.1007/s10924-019-01374-6.

[17] C.R. Álvarez-Chávez, D.L. Sánchez-Acosta, J.C. Encinas-Encinas, J. Esquer, P. QuintanaOwen, T.J. Madera-Santana, Characterization of Extruded Poly(lactic acid)/Pecan Nutshell Biocomposites, Int. J. Polym. Sci. 2017 (2017) 1–12. https://doi.org/10.1155/2017/3264098.

[18] L.W. Gallagher, A.G. McDonald, The effect of micron sized wood fibers in wood plastic composites, Maderas. Cienc. y Tecnol. 15 (2013) 0–0. https://doi.org/10.4067/S0718221X2013005000028.

[19] N. Suaduang, S. Ross, G.M. Ross, S. Pratumshat, S. Mahasaranon, Effect of spent coffee grounds filler on the physical and mechanical properties of poly(lactic acid) bio-composite films, Mater. Today Proc. 17 (2019) 2104–2110. https://doi.org/10.1016/j.matpr.2019.06.260.

[20] T. Huber, M. Misra, A.K. Mohanty, The effect of particle size on the rheological properties of polyamide 6/biochar composites, AIP Conf. Proc. 1664 (2015) 6–10. https://doi.org/10.1063/1.4918500.

[21] Y. Zheng, Z. Fu, D. Li, M. Wu, Effects of ball milling processes on the microstructure and rheological properties of microcrystalline cellulose as a sustainable polymer additive, Materials (Basel). 11 (2018) 1–13. https://doi.org/10.3390/ma11071057.

[22] A. Isa, J. Minamino, Y. Kojima, S. Suzuki, H. Ito, R. Makise, M. Okamoto, T. Endo, The Influence of Dry-Milled Wood Flour on The Physical Properties of Wood Flour/Polypropylene Composites, J. Wood Chem. Technol. 36 (2016) 105–113. https://doi.org/10.1080/02773813.2015.1083583.

[23] C.G. Silva, P.A.L. Campini, D.B. Rocha, D.S. Rosa, The influence of treated eucalyptus microfibers on the properties of PLA biocomposites, Compos. Sci. Technol. 179 (2019) 54–62. https://doi.org/10.1016/j.compscitech.2019.04.010.

[24] V. Baheti, J. Militky, M. Marsalkova, Mechanical properties of poly lactic acid composite films reinforced with wet milled jute nanofibers, Polym. Compos. 34 (2013) 2133–2141. https://doi.org/10.1002/pc.22622.

[25] S. Bhagia, R.R. Lowden, D. Erdman, M. Rodriguez, B.A. Haga, I.R.M. Solano, N.C. Gallego, Y. Pu, W. Muchero, V. Kunc, A.J. Ragauskas, Tensile properties of 3D-printed wood-filled PLA materials using poplar trees, Appl. Mater. Today. 21 (2020) 100832. https://doi.org/10.1016/j.apmt.2020.100832.

[26] R. Avolio, V. Graziano, Y.D.F. Pereira, M. Cocca, G. Gentile, M.E. Errico, V. Ambrogi,

M. Avella, Effect of cellulose structure and morphology on the properties of poly(butylene succinate-co-butylene adipate) biocomposites, Carbohydr. Polym. 133 (2015) 408–420. https://doi.org/10.1016/j.carbpol.2015.06.101.

[27] R. Prem chand, Y.P. Ravitej, K.M. Chandrasekhar, H. Adarsha, J.V. Shivamani kanta, M.

Eliminato: 15

Eliminato: 16

Eliminato: [19

Spostato in su [5]:] S. Agustin-Salazar, P. Cerruti, L.Á. Medina-Juárez, G. Scarinzi, M. Malinconico, H. SotoValdez, N. Gamez-Meza, Lignin and holocellulose from pecan nutshell as reinforcing fillers in poly (lactic acid) biocomposites, Int. J. Biol. Macromol. 115 (2018) 727– 736. https://doi.org/10.1016/j.ijbiomac.2018.04.120.¶

Eliminato: [20

Eliminato: 21

Eliminato: 17

Eliminato: 22

Eliminato: 23

Eliminato: 18

Eliminato: 24

Eliminato: 25

Eliminato: 26

Eliminato: 27

Eliminato: 28

Veerachari, R. Ravi kumar, Abhinandan, Characterization of banana and E glass fiber reinforced hybrid epoxy composites, Mater. Today Proc. 46 (2021) 9119–9125. https://doi.org/10.1016/j.matpr.2021.05.402.

[28] M. Cocca, M.L. Di Lorenzo, M. Malinconico, V. Frezza, Influence of crystal polymorphism on mechanical and barrier properties of poly(l-lactic acid), Eur. Polym. J. 47 (2011) 1073–1080. https://doi.org/10.1016/j.eurpolymj.2011.02.009.

[29] N. Vasanthan, O. Ly, Effect of microstructure on hydrolytic degradation studies of poly (l-lactic acid) by FTIR spectroscopy and differential scanning calorimetry, Polym. Degrad. Stab. 94 (2009) 1364–1372. https://doi.org/10.1016/j.polymdegradstab.2009.05.015.

[30] J.B. Engel, M. Mac Ginity, C.L. Luchese, I.C. Tessaro, J.C. Spada, Reuse of Different Agroindustrial Wastes: Pinhão and Pecan Nutshells Incorporated into Biocomposites Using Thermocompression, J. Polym. Environ. 28 (2020) 1431–1440. https://doi.org/10.1007/s10924-020-01696-w.

[31] C.L. Luchese, V.F. Abdalla, J.C. Spada, I.C. Tessaro, Evaluation of blueberry residue incorporated cassava starch film as pH indicator in different simulants and foodstuffs, Food Hydrocoll. 82 (2018) 209–218. https://doi.org/10.1016/j.foodhyd.2018.04.010.

[32] H. Long, Z. Wu, Q. Dong, Y. Shen, W. Zhou, Y. Luo, C. Zhang, X. Dong, Effect of polyethylene glycol on mechanical properties of bamboo fiber-reinforced polylactic acid composites, J. Appl. Polym. Sci. 136 (2019) 3–10. https://doi.org/10.1002/app.47709.

[33] S. Agustin-Salazar, N. Gamez-Meza, L.Á. Medina-Juárez, M. Malinconico, P. Cerruti, Stabilization of Polylactic Acid and Polyethylene with Nutshell Extract: Efficiency Assessment and Economic Evaluation, ACS Sustain. Chem. Eng. 5 (2017). https://doi.org/10.1021/acssuschemeng.6b03124.

[34] S. Agustin-Salazar, L.A. Medina-Juárez, H. Soto-Valdez, F. Manzanares-López, N. Gámez-Meza, Influence of the solvent system on the composition of phenolic substances and antioxidant capacity of extracts of grape (Vitis vinifera L.) marc, Aust. J. Grape Wine Res. 20 (2014) 208–213. https://doi.org/10.1111/ajgw.12063.

[35] F. Manzanarez-López, H. Soto-Valdez, R. Auras, E. Peralta, Release of α-Tocopherol from Poly(lactic acid) films, and its effect on the oxidative stability of soybean oil, J. Food Eng. 104 (2011) 508–517. https://doi.org/10.1016/j.jfoodeng.2010.12.029.

[36] S.L.B. Navarro, C.E.C. Rodrigues, Macadamia oil extraction methods and uses for the defatted meal byproduct, Trends Food Sci. Technol. 54 (2016) 148–154. https://doi.org/10.1016/j.tifs.2016.04.001.

[37] X. Zhuang, Z. Zhang, Y. Wang, Y. Li, The effect of alternative solvents to n-hexane on the green extraction of Litsea cubeba kernel oils as new oil sources, Ind. Crops Prod. 126 (2018) 340–346. https://doi.org/10.1016/j.indcrop.2018.10.004.

[38] F. Moccia, S. Agustin-Salazar, L. Verotta, E. Caneva, S. Giovando, G. D'Errico, L. Panzella, M. D'Ischia, A. Napolitano, Antioxidant properties of agri-food byproducts | and specific boosting effects of hydrolytic treatments, Antioxidants. 9 (2020) 1–22. https://doi.org/10.3390/antiox9050438.

[39] M. Kacuráková, P. Capek, V. Sasinková, N. Wellner, A. Ebringerová, FT-IR study of plant cell wall model compounds: pectic polysaccharides and hemicelluloses, Carbohydr. Polym. 43 (2000) 195–203. https://doi.org/10.1016/S0144-8617(00)00151-X.

[40] L.M. Ilharco, A.R. Garcia, J. Lopes da Silva, L.F. Vieira Ferreira, Infrared Approach to the Study of Adsorption on Cellulose: Influence of Cellulose Crystallinity on the Adsorption of Benzophenone, Langmuir. 13 (1997) 4126–4132. https://doi.org/10.1021/la962138u.

[41] Z. Ling, T. Wang, M. Makarem, M. Santiago Cintrón, H.N. Cheng, X. Kang, M. Bacher, A. Potthast, T. Rosenau, H. King, C.D. Delhom, S. Nam, J. Vincent Edwards, S.H. Kim, F. Xu, A.D. French, Effects of ball milling on the structure of cotton cellulose, Cellulose. 26 (2019) 305–328.

Eliminato: 29
Eliminato: 30
Eliminato: 31
Eliminato: 32
Eliminato: 33
Eliminato: 34
Eliminato: 35
Eliminato: 36
Eliminato: 37
Eliminato: 38
Eliminato: 39
Eliminato: 40
Eliminato: 41

https://doi.org/10.1007/s10570-018-02230-x.
[42] M. Schwanninger, J.C. Rodrigues, H. Pereira, B. Hinterstoisser, Effects of short-time vibratory ball milling on the shape of FT-IR spectra of wood and cellulose, Vib. Spectrosc. 36 (2004) 23–40. https://doi.org/10.1016/j.vibspec.2004.02.003.
[43] A.A. Vaidya, L.A. Donaldson, R.H. Newman, I.D. Suckling, S.H. Campion, J.A. Lloyd, K.D. Murton, Micromorphological changes and mechanism associated with wet ball milling of Pinus radiata substrate and consequences for saccharification at low enzyme loading, Bioresour. Technol. 214 (2016) 132–137. https://doi.org/10.1016/j.biortech.2016.04.084.
[44] A. Solikhin, Y.S. Hadi, M.Y. Massijaya, S. Nikmatin, Novel Isolation of Empty Fruit Bunch Lignocellulose Nanofibers Using Different Vibration Milling Times-Assisted Multimechanical Stages, Waste and Biomass Valorization. 8 (2017) 2451–2462. https://doi.org/10.1007/s12649-016-9765-0.
[45] U.J. Kim, S.H. Eom, M. Wada, Thermal decomposition of native cellulose: Influence on crystallite size, Polym. Degrad. Stab. 95 (2010) 778–781. https://doi.org/10.1016/j.polymdegradstab.2010.02.009.
[46] E.O. Ogunsona, M. Misra, A.K. Mohanty, Composites : Part A Impact of interfacial adhesion on the microstructure and property variations of biocarbons reinforced nylon 6 biocomposites, Compos. Part A. 98 (2017) 32–44. https://doi.org/10.1016/j.compositesa.2017.03.011.
[47] Y. Zheng, Z. Fu, D. Li, M. Wu, Effects of Ball Milling Processes on the Microstructure and Rheological Properties of Microcrystalline Cellulose as a Sustainable Polymer Additive, Materials (Basel). 11 (2018) 1057. https://doi.org/10.3390/ma11071057.
[48] O. Olejnik, A. Masek, J. Zawadziłło, Processability and Mechanical Properties of Thermoplastic Polylactide/Polyhydroxybutyrate (PLA/PHB) Bioblends, Materials (Basel). 14 (2021) 898. https://doi.org/10.3390/ma14040898.
[49] V. Nagarajan, A.K. Mohanty, M. Misra, Biocomposites with Size-Fractionated Biocarbon: Influence of the Microstructure on Macroscopic Properties, ACS Omega. 1 (2016) 636–647. https://doi.org/10.1021/acsomega.6b00175.
[50] V. Mazzanti, F. Mollica, A review of wood polymer composites rheology and its implications for processing, Polymers (Basel). 12 (2020) 1–23. https://doi.org/10.3390/polym12102304.
[51] A. Orue, A. Eceiza, A. Arbelaiz, The effect of sisal fiber surface treatments, plasticizer addition and annealing process on the crystallization and the thermo-mechanical properties of poly(lactic acid) composites, Ind. Crops Prod. 118 (2018) 321–333. https://doi.org/10.1016/j.indcrop.2018.03.068.
[52] L. Běhálek, M. Maršálková, P. Lenfeld, J. Habr, J. Bobek, M. Seidl, Study Of Crystallization Of Polylactic Acid Composites And Nanocomposites With Natural Fibres

Eliminato: 42

Eliminato: 43

Eliminato: 44

Eliminato: 45

Eliminato: 46

Eliminato: 47

Eliminato: 48

Eliminato: 49

Eliminato: 50

Eliminato: 51

Eliminato: 52

Eliminato: 53

Eliminato: 54

Eliminato: STUDY OF CRYSTALLIZATION OF POLYLACTIC ACID COMPOSITES AND NANOCOMPOSITES WITH NATURAL FIBRES BY DSC METHOD

By Dsc Method, in: NANOCON 2013. 5th Int. Conf., Technical University of Liberec, Brno, Czech Republic., 2013: pp. 1–6.
[53] L. Ferry, G. Dorez, A. Taguet, B. Otazaghine, J.M. Lopez-Cuesta, Chemical modification of lignin by phosphorus molecules to improve the fire behavior of polybutylene succinate, Polym. Degrad. Stab. 113 (2015) 135–143. https://doi.org/10.1016/j.polymdegradstab.2014.12.015.
[54] T. Tábi, S. Hajba, J.G. Kovács, Effect of crystalline forms (α′ and α) of poly(lactic acid) on its mechanical, thermo-mechanical, heat deflection temperature and creep properties, Eur. Polym. J. 82 (2016) 232–243. https://doi.org/10.1016/j.eurpolymj.2016.07.024.
[55] J. Chen, C. Deng, R. Hong, Q. Fu, J. Zhang, Effect of thermal annealing on crystal structure and properties of PLLA/PCL blend, J. Polym. Res. 27 (2020) 221. https://doi.org/10.1007/s10965-020-02206-1.
[56] V. Di Lisio, F. Sturabotti, I. Francolini, A. Piozzi, A. Martinelli, Effects of annealing above Tg on the physical aging of quenched PLLA studied by modulated temperature FTIR, J. Polym. Sci. Part B Polym. Phys. 57 (2019) 174–181. https://doi.org/10.1002/polb.24769.
[57] J. Zhang, Y. Duan, H. Sato, H. Tsuji, I. Noda, S. Yan, Y. Ozaki, Crystal modifications and properties of injection -molded poly (lactic acid) parts through annealing, J. AAraújo, R.M.R. Wellen, Annealing efficacy on PLA. thermal behavior of poly(L-lactic acid) revealed by infrared spectroscopy, Macromolecules. 38 (2005) 8012–8021. https://doi.org/10.1021/ma051232r.
[58] A. International, ASTM D648-18, Standard Test Method for Deflection Temperature of Plastics Under Flexural Load in the Edgewise Position, (n.d.). https://doi.org/10.1520/D0648-18.
[59] G. Li, B. Yang, W. Han, H. Li, Z. Kang, J. Lin, Tailoring the thermal and mechanical Sci. 138 (2021) 49648. https://doi.org/10.1002/app.49648.
[60] Q.F. Shi, H.Y. Mou, Q.Y. Li, J.K. Wang, W.H. Guo, Influence of heat treatment on the heat distortion temperature of poly(lactic acid)/bamboo fiber/talc hybrid biocomposites, J. Appl. Polym. Sci. 123 (2012) 2828–2836. https://doi.org/10.1002/app.34807.
[61] R.A. Bubeck, A. Merrington, A. Dumitrascu, P.B. Smith, Thermal analyses of poly(lactic acid) PLA and micro-ground paper blends, J. Therm. Anal. Calorim. 131 (2018) 309–316. https://doi.org/10.1007/s10973-017-6466-2.
[62] J. Wootthikanokkhan, T. Cheachun, N. Sombatsompop, S. Thumsorn, N. Kaabbuathong, N. Wongta, J. Wong-On, S.I. Na Ayutthaya, A. Kositchaiyong, Crystallization and thermomechanical properties of PLA composites: Effects of additive types and heat treatment, J. Appl. Polym. Sci. 129 (2013) 215–223. https://doi.org/10.1002/app.38715.
[63] J. Móczó, B. Pukánszky, Polymer micro and nanocomposites: Structure, interactions, properties, J. Ind. Eng. Chem. 14 (2008) 535–563. https://doi.org/10.1016/j.jiec.2008.06.011.
[64] B. Pukánszky, Influence of interface interaction on the ultimate tensile properties of polymer composites, Composites. 21 (1990) 255–262. https://doi.org/10.1016/00104361(90)90240-W.
[65] D. Battegazzore, S. Bocchini, J. Alongi, A. Frache, Plasticizers, antioxidants and reinforcement fillers from hazelnut skin and cocoa by-products : Extraction and use in PLA and PP, Polym. Degrad. Stab. (2014). https://doi.org/10.1016/j.polymdegradstab.2014.03.003.
[66] M.X. Li, S.H. Kim, S.W. Choi, K. Goda, W. Il Lee, Effect of reinforcing particles on Insights on mechanical, thermomechanical and crystallinity characters, MOMENTO. 2021 (2021) 1–17. https://doi.org/10.15446/mo.n62.89099.¶ [62

Eliminato: 55
Eliminato: 56
Eliminato: 57
Eliminato:).
Eliminato: 58
Eliminato: 59
Eliminato: 60
Eliminato: [61] C.B.B. Luna, D.D. Siqueira, E.M.
Eliminato: 63
Eliminato: 64
Eliminato: 65

Eliminato: 66

Eliminato: 67

Eliminato: 68

Eliminato: 69

hydrolytic degradation behavior of poly (lactic acid) composites, Compos. Part B Eng. 96 (2016) 248–254. https://doi.org/10.1016/j.compositesb.2016.04.029.